Geological Magazine

www.cambridge.org/geo

Original Article

Cite this article: Maldonado R, Solari LA, Morán-Chen H, and Ortiz-Joya GA. Origin of the internal basement massif of the Guatemala Suture Zone: evidence from U-Pb geochronology and Sm-Nd and Lu-Hf isotope systematics. *Geological Magazine* **161**(e15): 1–16. https://doi.org/10.1017/S0016756824000347

Received: 13 September 2023
Revised: 28 September 2024
Accepted: 30 September 2024

Keywords:
Zircon; geochronology; isotope systematic; Chuacús complex; magmatism; Rodinia; Pangea

Corresponding author:
Roberto Maldonado;
Email: robertom@geologia.unam.mx

Origin of the internal basement massif of the Guatemala Suture Zone: evidence from U-Pb geochronology and Sm-Nd and Lu-Hf isotope systematics

Roberto Maldonado[1], Luigi A. Solari[2], Helen Morán-Chen[3] and Guillermo A. Ortiz-Joya[4]

[1]Instituto de Geología, Universidad Nacional Autónoma de México, Mexico City, Mexico; [2]Instituto de Geociencias, Universidad Nacional Autónoma de México, Campus Juriquilla, Querétaro, Mexico; [3]Centro Universitario del Norte, Universidad de San Carlos de Guatemala, Cobán, Guatemala and [4]School of Earth Atmosphere and Environment, Monash University, Clayton, Australia

Abstract

The origin of eclogite-bearing granitoid gneisses and metapelites of the Chuacús Complex is investigated. This complex represents the internal basement massif of the Guatemala Suture Zone, a part of the western North America–Caribbean plate boundary. LA-ICP-MS U-Pb and trace element zircon data are combined with whole-rock Sm-Nd and Lu-Hf isotopes to re-evaluate granitoid petrogenesis and inquire into the sedimentary record. New granitoid ages of ca. 1030–1010 Ma are reported, adding to those already known of ca. 1100, 990 and 225 Ma. Stenian A-type granitoids within the bimodal Cubulco unit formed by mixing of magmas derived from late Palaeoproterozoic crust and mantle-derived melts produced in an extensional setting during Rodinia assembly. During the Tonian, an extended (or later) period of extensional tectonics produced peraluminous granitoids (Pachajob gneiss) by anatexis of rejuvenated late Mesoproterozoic crust. After a hiatus encompassing most of the Neoproterozoic, marine sedimentation occurred between the Ediacaran and the early Palaeozoic as recorded by the Palibatz schist, a sequence formed by detritus sourced from peri-Gondwanan continental areas. No evidence of middle to late Palaeozoic magmatism or sedimentation was found in the studied area. Late Triassic granitoids (Agua Caliente unit) were produced by mixing melts from late Mesoproterozoic crust with enriched mantle magmas in response to post-collisional thinning during the western Pangea breakup. This extensional stage led to considerable thinning of the Chuacús crust and its evolution into a passive margin that would be prone to subduct during the Cretaceous.

1. Introduction

The Guatemala Suture Zone (GSZ) (Brueckner *et al.* 2009; Flores *et al.* 2013) is a composite east-west trending, left-lateral strike-slip zone that defines the current boundary between the North American and Caribbean plates in Guatemala (Fig. 1a). This zone has been active since at least the Miocene (Rogers & Mann, 2007; Authemayou *et al.* 2011; Obrist-Farner *et al.* 2020), but its geological record reflects processes of both accretionary and collisional orogenesis dating back to the Cretaceous and consistent with the development of the Circum-Caribbean suture system (Draper *et al.* 1996; Harlow *et al.* 2004; García-Casco *et al.* 2006; Maresch *et al.* 2009). Since the magnitude of lateral displacement between different crustal blocks within the GSZ during the Cenozoic is mostly unknown, the along-strike variation in the overall architecture of the Cretaceous orogen is thus far uncertain.

The GSZ contains a complex mixture of continental margin rocks and remnants of oceanic lithosphere, some of which enclose eclogite, blueschist and other high-pressure (HP) metamorphic rocks spanning in age from Berriasian to Campanian (Harlow *et al.* 2004; Brueckner *et al.* 2009; Yui *et al.* 2010; Martens *et al.* 2012; Flores *et al.* 2013; Maldonado *et al.* 2018a). Of special interest is the occurrence of gneiss-hosted eclogites in the Chuacús Complex (Ortega-Gutiérrez *et al.* 2004), directly adjacent to the Motagua fault zone, which provide evidence that the GSZ includes a portion of deeply subducted continental crust. Recent research has focused on investigating the timing, conditions and context of this process in the area (Martens *et al.* 2012; Martens *et al.* 2017; Maldonado *et al.* 2016, 2018a, 2018b). At the same time, the question arises as to what the origin of the subducted crust is and what relationships it has with other pre-Cretaceous terranes of the Circum-Caribbean region. Most of these terranes cover an area throughout Mexico, Central America and northern South America and are commonly referred to as 'peri-Gondwanan' terranes (e.g. Oaxaquia, Maya block, Chortí block

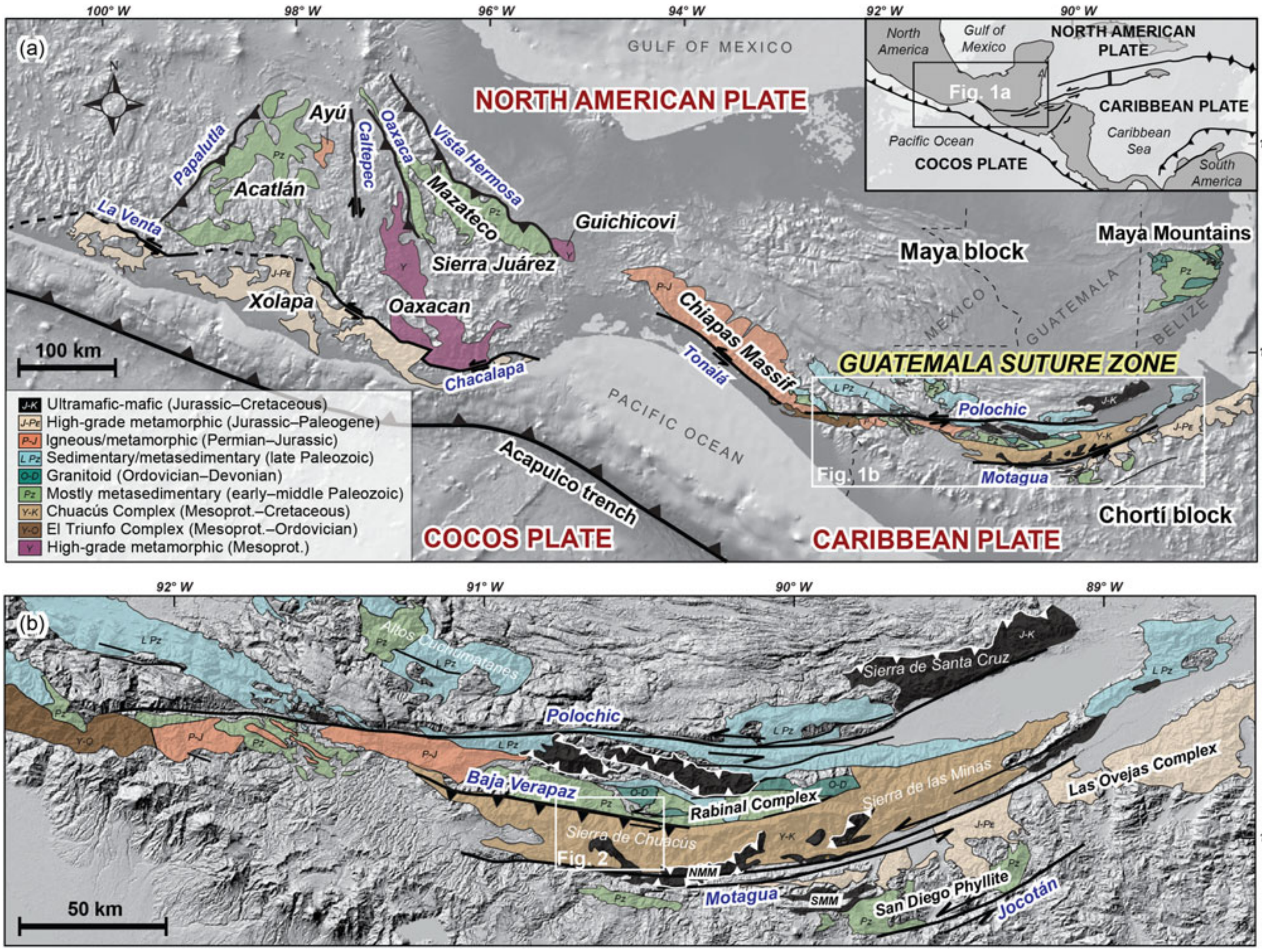

Figure 1. Geological setting of the Guatemala Suture Zone with inset of location within the Circum-Caribbean region. (a) Tectonic overview of the North American-Caribbean-Cocos triple junction region showing the location of the Guatemala Suture Zone (white rectangle) as well as major basement exposures of southern Mexico, Guatemala and Belize (modified after Kesler *et al*. 1970; Anderson *et al.* 1973; Ortega-Gutiérrez *et al.* 2007, 2018; Ratschbacher *et al.* 2009; Martens *et al*. 2010; Weber *et al.* 2018). (b) Geological map of the Guatemala Suture Zone indicating the study area. Relevant basement units are labelled with black cursives, whereas major fault zones are indicated by bold lines and blue cursives. NMM: North Motagua mélange; SMM: South Motagua mélange.

and Mérida Andes). In particular, the kinship between the Chuacús Complex and the composite continental Maya (North America) and Chortí (Caribbean) blocks (Dengo, 1969; Donnelly *et al.* 1991) remains mostly speculative. Based on apparent lithostratigraphic similarities and the tectonic arrangement of the GSZ resembling a Cretaceous Himalaya-style orogen (O'Brien, 2019), some authors have suggested that the Chuacús Complex originally formed part of the Maya block (Ratschbacher *et al.* 2009; Martens *et al.* 2017; Maldonado *et al.* 2018a). Accordingly, the current paradigm is that the Maya's margin was subjected to southward subduction during the Cretaceous, a model that requires a plate configuration similar to that of prevailing palinspastic reconstructions (e.g. Pindell *et al.* 2012). However, interpretations about the origin and evolution of the Chuacús Complex have changed considerably over the last two decades. Research is moving towards a more comprehensive understanding of its protracted evolution as well as palaeogeographic connections and significance.

Most previous works combine either petrologic or structural analysis with geochronological data (Ortega-Gutiérrez *et al.* 2004; Ratschbacher *et al.* 2009; Martens *et al.* 2012; Maldonado *et al.* 2018a, 2018b), and only a few studies integrate geochemical, isotopic and geochronological information (Solari *et al.* 2011; Maldonado *et al.* 2023), essential to propose petrogenetic interpretations. This has resulted in a still sparse and incomplete database for the Chuacús Complex. In a couple of recent studies, we focused on both the petrogenesis of eclogite protoliths (Maldonado *et al.* 2023) and the general characterization of the hosting granitoid gneisses (Maldonado *et al.* 2018b). In this contribution, we integrate and complete the existing database, coupling new U-Pb and trace element zircon data with whole-rock Sm-Nd and Lu-Hf isotope analyses of metagranitoids and metapelites from the Chuacús Complex, in order to refine understanding of the petrogenesis, sedimentary record and nature of the tectonothermal events in this region and its role in the Rodinia and Pangea supercontinent cycles.

2. Geological setting

2.a. The Guatemala suture zone

The GSZ includes the Polochic, Baja Verapaz, Motagua and Jocotán fault zones (Fig. 1b) that currently define diffuse tectonic

https://doi.org/10.1017/S0016756824000347 Published online by Cambridge University Press

limits, bounding distinctive crystalline basement units with ages varying from the Mesoproterozoic to the Jurassic (Ortega-Gutiérrez *et al.* 2007). The updated pre-Cretaceous lithostratigraphy of this area was recently summarized in Maldonado *et al.* (2023), so only a brief overview is given below.

Between the Polochic and Baja Verapaz fault zones, Neoproterozoic or early Palaeozoic low-grade metasediments (San Gabriel Unit) and cross-cutting deformed Ordovician-Silurian granitoids (Rabinal Granite) compose the Rabinal Complex of Maya affinity (Ratschbacher *et al.* 2009; Ortega-Obregón *et al.* 2008; Solari *et al.* 2013; Solari *et al.* 2009). This sequence is unconformably overlain by continental sedimentary rocks of the Carboniferous Sacapulas Formation (Santa Rosa Group) (Ortega-Obregón *et al.* 2008; Solari *et al.* 2009). Altogether, these units are overthrust in places by ultramafic slices of the Baja Verapaz ophiolitic unit, which represent remnants of the Caribbean oceanic crust, formed in the Jurassic-Cretaceous by mid-ocean ridge activity and intraoceanic subduction (Giunta *et al.* 2002; Beccaluva, 1995). The southern limit of the Rabinal Complex corresponds to the Baja Verapaz fault zone, a south-southwest-dipping system with sinistral transpressive kinematics developed during the Late Cretaceous (Ortega-Obregón *et al.* 2008), along which the Rabinal Complex is in thrust contact with the eclogite-bearing Chuacús Complex (Ortega-Gutiérrez *et al.* 2004). Recent studies have shown that the Chuacús Complex recorded a protracted evolution since the Mesoproterozoic, including several pulses of magmatism (see Section 2.b below). This continental HP belt is bounded to the south by the left-lateral Motagua fault system, where it is tectonically overlain by serpentinite mélange wedges (North Motagua mélange) that are part of a typical collisional flower structure (Giunta *et al.* 2002). The juxtaposition of the Chuacús Complex and the North Motagua mélange occurred before the latest Cretaceous (Martens *et al.* 2012); however, the original spatial relationships were later disrupted by recent fault activity. Serpentinite mélanges north and south of the Motagua fault zone include blocks of HP moderate- to low-temperature metamorphic rocks, recording a process of oceanic subduction throughout the Cretaceous (Harlow *et al.* 2004; Tsujimori *et al.* 2006; Brueckner *et al.* 2009; Yui *et al.* 2010; Flores *et al.* 2013). The Las Ovejas Complex and the San Diego Phyllite are the southernmost basement units of the GSZ, exposed from the Motagua to the Jocotán fault zone and traditionally assigned to the Chortí block (Donnelly *et al.* 1991). These units are tectonically juxtaposed and record independent geological evolutions. The Las Ovejas Complex is an assemblage of Jurassic to Cretaceous metaigneous and metasedimentary rocks and Cenozoic plutons that experienced amphibolite-facies metamorphism in the late Eocene, whereas the San Diego Phyllite consists of post-Cambrian low-grade metasediments metamorphosed in the Triassic (Torres de León *et al.* 2012).

2.b. The Chuacús complex

The Chuacús Complex forms the internal basement massif of the GSZ, containing the region's deepest piece of continental crust and the oldest rocks known so far in Guatemala (Maldonado *et al.* 2023). It consists of an arcuate, ~220 km long metamorphic belt that includes an eclogite-bearing continental sequence (hereafter referred to as the HP suite) exposed along the Palibatz–Rabinal transect of the Sierra de Chuacús (Fig. 2). The metamorphism of the HP suite reflects a process of continental subduction and collision spanning from middle to Late Cretaceous (Martens *et al.* 2012; Maldonado *et al.* 2018a). The limits of the HP suite are not well known, but eclogite relicts have not been reported in other sectors of the massif (e.g. Sierra de las Minas; Fig. 1b). Since the predominant structural trend in the Sierra de Chuacús is defined by a NW-SE-striking, SW-dipping axial-plane foliation, the across-strike extension of the HP suite might be controlled by NE-directed thrust stacking and erosion that left deeper levels exposed in this area (Fig. 2). Its along-strike continuation is interrupted to the northwest and southeast by the Baja Verapaz and Motagua fault zones.

In general, the HP suite can be described in terms of a metaigneous group including granitoid gneiss, amphibolite and retrogressed eclogite and a metasedimentary group of interlayered mica schist and paragneiss, marble, quartzite and calc-silicate rocks (Fig. 2) (cf. Martens *et al.* 2017). However, recent improvements in the geological database allow to define some informal lithodemic units, most of which still lack a cartographic representation, and thus, only their type localities are shown (triangles) in Figure 2:

1) ***Palibatz schist***: consists of a garnet mica schist widely exposed in the southern Sierra de Chuacús, typically occupying a structurally upper position within the HP suite (Fig. 2). This unit includes coarse-grained layers containing the diagnostic HP assemblage garnet + phengite + kyanite + rutile (Ortega-Gutiérrez *et al.* 2004; Maldonado *et al.* 2018b). Maldonado *et al.* (2018b) obtained a garnet/whole-rock Lu-Hf age of 96 ± 2 Ma, as well as ca. 74 Ma U-Pb ages from late-stage zircon and monazite. Detrital zircon U-Pb data indicate post-Cryogenian (< ca. 690 Ma) deposition of the sedimentary protolith of this unit, whereas its chemical features suggest hemipelagic sedimentation and provenance from mature continental crust (Solari *et al.* 2011).

2) ***Pachajob gneiss***: is a folded and locally migmatized granitic gneiss exposed about 3 km west of the Pachajob village. This unit is structurally below the Palibatz schist and contains a HP paragenesis including Ca-rich garnet + phengite + rutile. U-Pb zircon dating determined the protolith crystallization age of the Pachajob gneiss at ca. 990 Ma (Maldonado *et al.* 2018b). This rock is high-silica and peraluminous in composition, and its trace element concentrations are consistent with a protolith formed by anatexis of a high-grade metamorphic crust (Maldonado *et al.* 2018b).

3) ***Cubulco unit***: is composed of variably deformed metagranitoids and subordinated amphibolite with eclogite relicts. It is well-exposed southwest of Cubulco town, in the northern Sierra de Chuacús, occupying an intermediate structural position within the HP suite. The original intrusive relationships between mafic dikes and host metagranitoids, as well as relic magmatic textures overgrown by HP minerals, are visible in the less deformed portions. However, diagnostic HP mineral assemblages are not always recognizable in the Cubulco unit. Granitic protoliths formed at ca. 1100 Ma, and their relatively high abundances of high-field-strength elements (HFSE) suggest a precursor magma sourced from an enriched mantle (Maldonado *et al.* 2018b). Recently, Maldonado *et al.* (2023) have reported U-Pb zircon ages between 1098 ± 46 and 1026 ± 29 Ma for OIB-like eclogite protoliths from the Tres Cruces–Palibatz sector, suggesting that the Cubulco unit constitutes a bimodal magmatic suite, probably related to intraplate magmatism.

4) ***Agua Caliente unit***: comprises a sequence of HP metagranitoids, retrogressed eclogites and amphibolites, well-exposed along the gorge of the Agua Caliente river, where it is structurally below the Palibatz schist and probably hosted by the Cubulco unit. This unit displays variable degrees of partial melting and deformation. Metagranitoids range from massive megacrystic

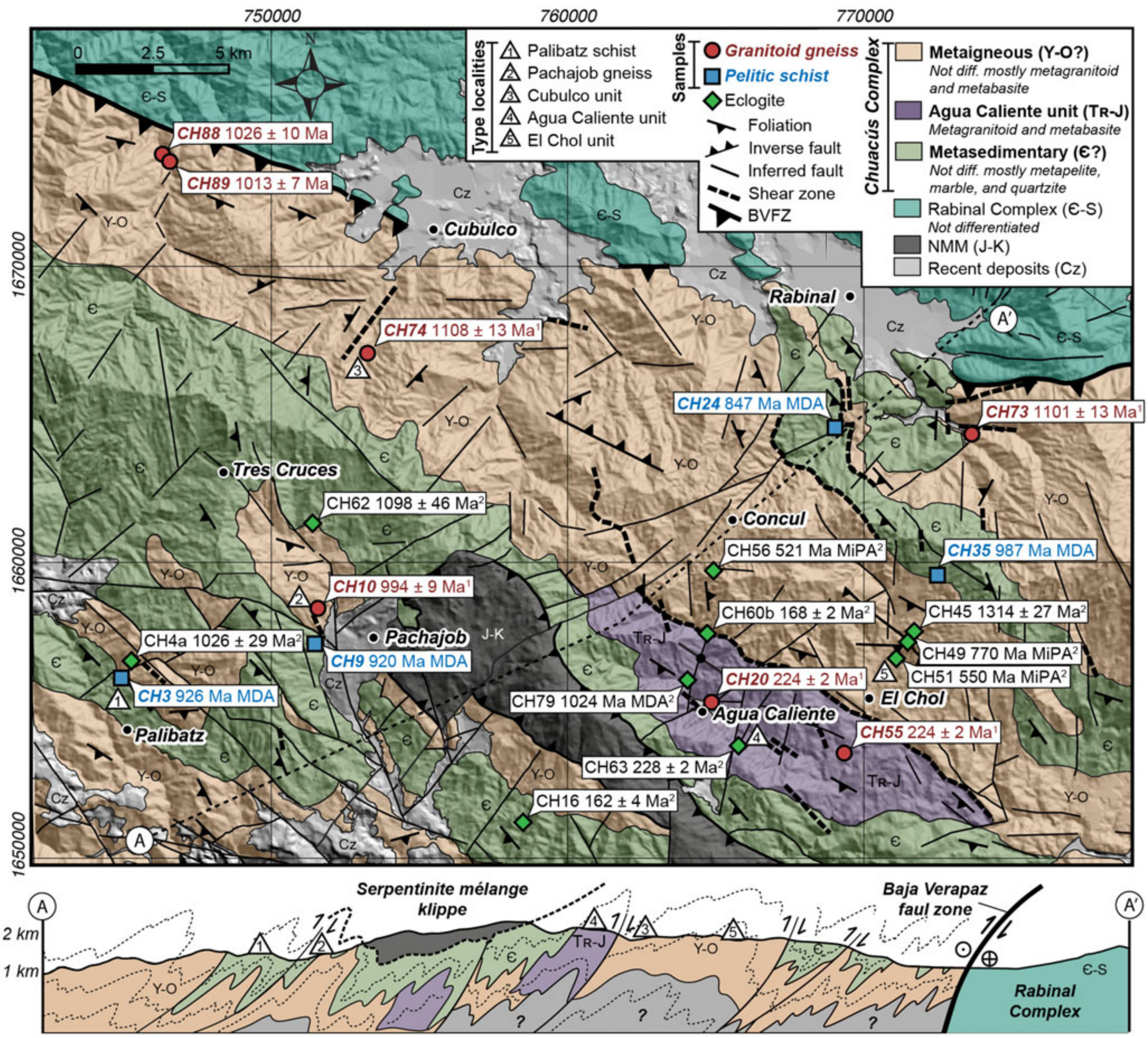

Figure 2. Simplified geological map and interpretative section of the Chuacús high-pressure suite exposed in the Sierra de Chuacús (modified after Maldonado *et al.* 2018b, 2018a). Geometric symbols highlight sample locations, eclogite occurrences and type localities of relevant lithodemic units in the area. Sample labels, including previously studied eclogites, are shown together with their corresponding U-Pb zircon ages in million years. Ages marked with superscripts were obtained previously by 1: Maldonado *et al.* (2018a) and 2: Maldonado *et al.* (2023). MDA: maximum depositional age; MiPA: minimum protolith age. BVFZ: Baja Verapaz fault zone; NMM: North Motagua mélange.

bodies to flaser gneiss, with mineral assemblages including Ca-rich garnet + epidote + phengite + rutile. Eclogite occurs as enclaves or lenses aligned subparallel to the foliation planes and range from pristine to strongly amphibolitized or albitized. Protolith ages of metagranitoids and eclogitized metabasites from this unit range from ca. 230 to 210 Ma (Solari *et al.* 2011; Martens *et al.* 2012; Maldonado *et al.* 2018b, 2023), thus constituting a Late Triassic bimodal suite. U-Pb zircon data and geochemistry of the Agua Caliente unit suggest an origin related to variable participation of an enriched mantle/crustal source and a contribution of Mesoproterozoic continental material (Maldonado *et al.* 2023). The HP suite also includes MORB-like eclogites with probable Jurassic (ca. 170–160 Ma) protoliths (Maldonado *et al.* 2023) that are considered part of the Agua Caliente unit.

5) ***El Chol unit***: consists of a polymetamorphic sequence of strongly retrogressed eclogite (amphibolite), omphacite-bearing gneiss, as well as metre-scale leucosome layers and deformed pegmatites, which lies structurally below the Agua Caliente and Cubulco units. This sequence is the structurally lowest level within the HP suite where eclogite relics are clearly preserved. The polymetamorphic character of the El Chol unit prevents a conclusive determination of protolith ages. Eclogite protoliths may have formed in two stages, at ca. 1310 and 1030 Ma (Maldonado *et al.* 2023), but zircon from these rocks show complex U-Pb spectra, with main age populations at the Ediacaran (ca. 600 Ma), the late Silurian (ca. 420 Ma) and the Late Triassic (ca. 220 Ma). The youngest group is related to the widespread migmatization of this unit (Solari *et al.* 2011; Maldonado *et al.*

https://doi.org/10.1017/S0016756824000347 Published online by Cambridge University Press

Table 1. Studied samples from the Chuacús high-pressure suite

Sample	Location (x y)*		Unit/locality	Rock type	Analytical data†	Previous work
CH10	751795	1657458	Pachajob gneiss	Granitoid gneiss	1, 2	Maldonado *et al.* (2018b)
CH20	764406	1655182	Agua Caliente unit	Granitoid gneiss	1, 2	Maldonado *et al.* (2018b)
CH55	768541	1654328	Agua Caliente unit	Metagranite	1, 2	Maldonado *et al.* (2018b)
CH73	772855	1664651	Cubulco unit	Granitoid gneiss	1, 2	Maldonado *et al.* (2018b)
CH74	752100	1667216	Cubulco unit	Metagranite	1, 2	Maldonado *et al.* (2018b)
CH88	746240	1673715	Cubulco unit	Granitoid gneiss	1, 2, 3	–
CH89	746420	1673614	Cubulco unit	Granitoid gneiss	1, 2, 3	–
CH3	744733	1656116	Palibatz schist	Pelitic schist	1, 3	–
CH9	751794	1657265	Palibatz schist	Pelitic schist	1, 3	Maldonado *et al.* (2018a)
CH24	769321	1664886	Northern Chuacús	Pelitic schist	1, 3	Maldonado *et al.* (2016)
CH35	772269	1659635	Northern Chuacús	Pelitic schist	1, 3	Maldonado *et al.* (2016)

*WGS84 UTM coordinates (15N).
†Analytical data presented in this study: 1 = Sm-Nd and Lu-Hf whole-rock isotopes; 2 = zircon trace element data; 3 = zircon U-Pb data.

2023). Some eclogites from the El Chol unit show subduction geochemical signatures and could have formed in an extensional arc setting, whereas others have OIB-type compositions similar to the Cubulco eclogites.

3. Samples, methods and data handling

3.a. Samples

Seven granitoid gneiss samples from the Palibatz-Rabinal transect of the Sierra de Chuacús were used in this study. Five of them correspond to previously studied samples in Maldonado *et al.* (2018b), and the other two (CH88 and CH89) were collected ca. 10 km northwest of Cubulco, along the trace of the Baja Verapaz fault zone (Fig. 2). The term 'granitoid' is used hereafter to refer to these variably deformed rocks (Maldonado *et al.* 2018b). Additionally, two metapelite samples (CH3 and CH9) from the Palibatz schist, and two others (CH24 and CH35) from a metapelite sequence exposed in the northern flank of the Sierra de Chuacús were studied. Sample CH3 was collected from an outcrop in the Tanilar River, ca. 2 km north of Palibatz. Sample CH9 is from the Saltán River near the Pachajob village and was previously studied by Maldonado *et al.* (2018a). Samples CH24 and CH35 were obtained from outcrops along the El Chol-Rabinal road in the Pachirax creek and around El Apazote village; both samples were investigated earlier by Maldonado *et al.* (2016). Sample information is summarized in Table 1.

3.b. Zircon U-Pb isotope and chemical analysis

Zircon crystals were employed from all four metapelite samples and two granitoids (CH88 and CH89) for U-Pb isotope analysis using laser ablation inductively coupled plasma mass spectrometry (LA-ICP-MS). Trace element concentrations in zircon from all seven granitoid samples were also determined in situ by LA-ICP-MS. Standard errors associated with individual analyses are reported at 2s level. Analytical procedures and results are presented in the online Supplementary Material at http://journals.cambridge.org/geo.

U-Pb discordance is the log ratio distance to the maximum likelihood composition on the concordia line (Vermeesch, 2021). Adaptive kernel density estimates (Vermeesch, 2012) were used to evaluate the age spectra and to determine maximum depositional ages for each metasedimentary sample. For this purpose, a discordance filter based on the log ratio distance to the concordia composition, a discordance cut-off value of 10% and single-grain concordia ages were used, as suggested by Vermeesch (2021).

3.c. Sm-Nd and Lu-Hf isotope analysis

All samples were used for whole-rock Sm-Nd and Lu-Hf isotope dilution analysis. Initial $^{143}Nd/^{144}Nd$ and $^{176}Hf/^{177}Hf$ isotope data for granitoid samples were recalculated at the crystallization ages, determined by U-Pb zircon dating (Maldonado *et al.* 2018b; this work). For metapelites from the Palibatz schist and northern Chuacús, an age of 500 Ma was assumed based on U-Pb zircon data obtained in this work. A description of sample processing and isotope analytical methods is presented in the online Supplementary Material at http://journals.cambridge.org/geo.

Depleted mantle (T_{DM}) Sm-Nd model ages were calculated using present-day isotopic values of Liew and Hofmann (1988) and the decay constant (λ) value for ^{147}Sm of Lugmair and Marti (1978). For Lu-Hf, T_{DM} model ages were determined according to the present-day values of Vervoort *et al.* (2000) and the $\lambda^{176}Lu$ value of Scherer *et al.* (2001) and Söderlund *et al.* (2004). Epsilon (ε) Nd and εHf values were calculated using chondritic uniform reservoir (CHUR) values after Bouvier *et al.* (2008).

4. Results

4.a. U-Pb zircon geochronology

4.a.1. Cubulco unit

Samples from the Cubulco unit correspond to concordant layers, tens of metres thick, within a mylonitic gneiss sequence affected by the Baja Verapaz fault zone. Sample CH88 is a leucocratic granitoid gneiss with plagioclase augen, quartz, white mica, K-feldspar ($\leq$ 5%), biotite, epidote, titanite, carbonate, apatite and zircon. Zircon crystals occur as elongated prisms (up to 500 μm long) displaying concentric and oscillatory zoning in cathodoluminescence (CL) images (Fig. 3). Forty-seven analyses from this sample yield concordant to moderately discordant ($\leq$ 22%) results. A

https://doi.org/10.1017/S0016756824000347 Published online by Cambridge University Press

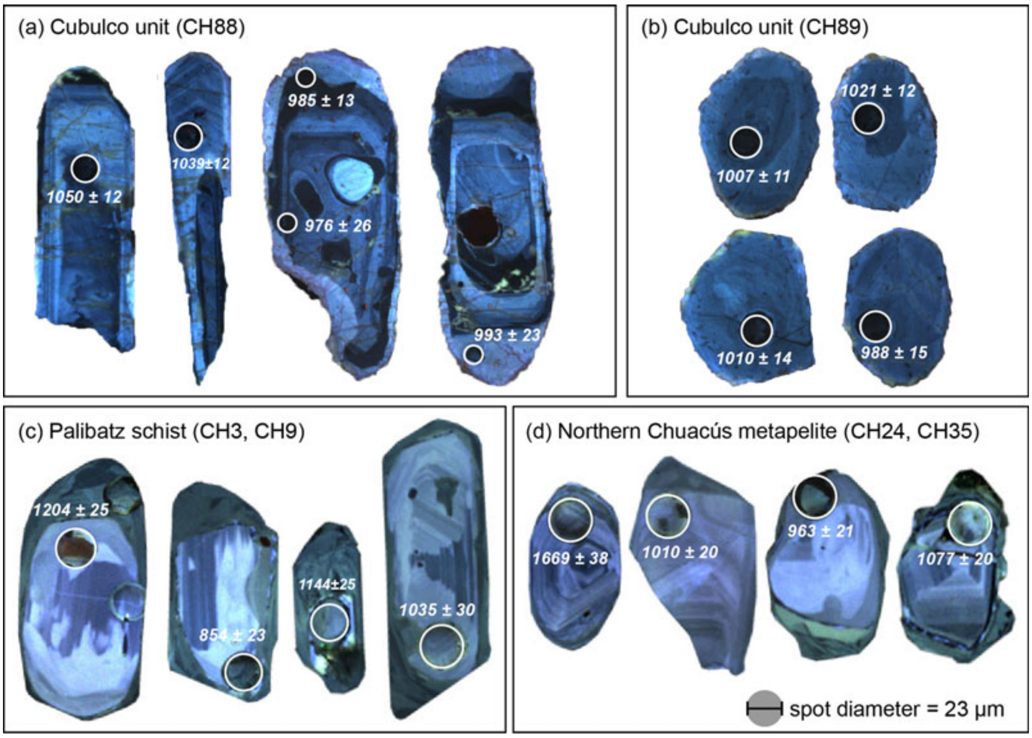

Figure 3. Post-ablation cathodoluminescence images of representative zircon crystals from (a–b) the Cubulco unit, (c) the Palibatz schist and (d) the northern Chuacús metapelite. Laser spots (white open circles) are labelled with the corresponding $^{206}Pb/^{238}U$ ages in million years. Note that each zircon is shown at a different scale.

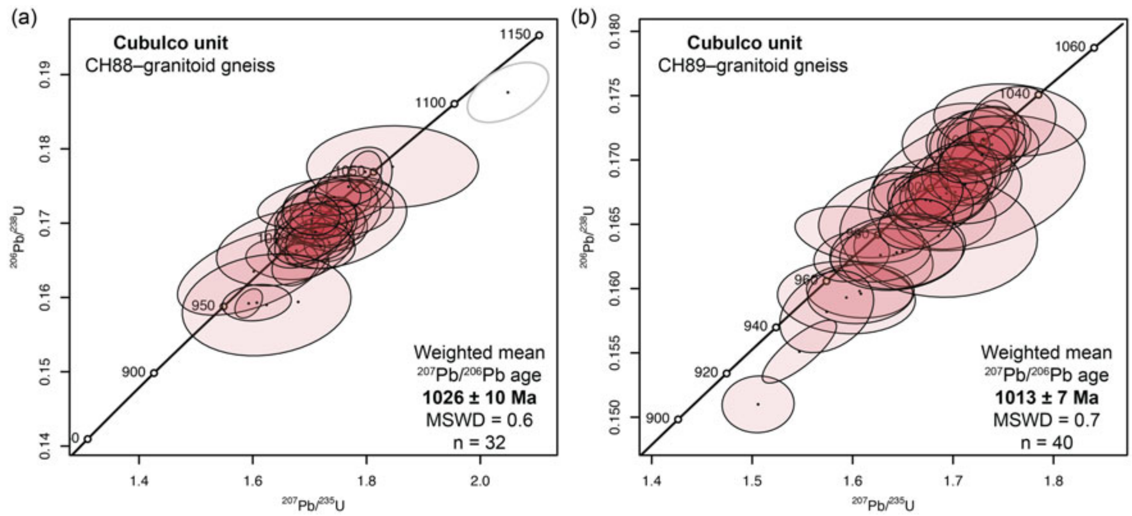

Figure 4. U-Pb zircon isotope data of granitoid gneisses from the Cubulco unit. (a–b) Wetherill concordia diagrams plotted with error ellipses at the 2σ level (MSWD = mean square of the weighted deviates for age homogeneity or isochron fit). Grey open ellipses were discarded for the upper intercept age calculation.

group of 32 analyses with discordances below 5% show a spread along concordia by ca. 100 m.y. and provide a weighted mean $^{207}Pb/^{206}Pb$ age of 1026 ± 10 Ma (MSWD = 0.6) (Fig. 4a). One slightly discordant date at ca. 1100 Ma is interpreted as inherited.

Sample CH89 is a mesocratic granitoid gneiss that consists of plagioclase, quartz, white mica, epidote, K-feldspar (≤ 10%) and Fe-Ti oxide, with minor amounts of titanite, garnet, calcite, zircon and apatite. Zircon occurs as slightly rounded equant grains (up to 400 µm in size) with subtle concentric zoning. Forty-five analyses from this sample are concordant to slightly discordant (≤ 15%) and reflect a small amount of Pb loss. Forty analyses with discordances below 5 % produce a weighted mean $^{207}Pb/^{206}Pb$ age of 1013 ± 7 Ma (MSWD = 0.7) (Fig. 4b).

4.a.2. Palibatz schist

Samples from the Palibatz schist are coarse-grained metapelites that contain quartz, phengite, garnet and kyanite, as well as accessory minerals including rutile, Fe-Ti oxide, monazite, zircon and apatite. Zircon grains are variable in size and morphology; most of them include detrital cores displaying concentric, oscillatory and planar zoning patterns with dark overgrowth rims (Fig. 3). One hundred and eighty-six analyses were collected on 181 zircon grains from sample CH3 (Palibatz), of which 5 grains were double-analysed for core-rim dates. Most zircons are highly discordant (>30%) and scattered, reflecting distinct discordia trends with lower intercept ages between 150 and 50 Ma (Fig. 5a). Only 15 analyses passed a discordance filtering of −2–10%, which

https://doi.org/10.1017/S0016756824000347 Published online by Cambridge University Press

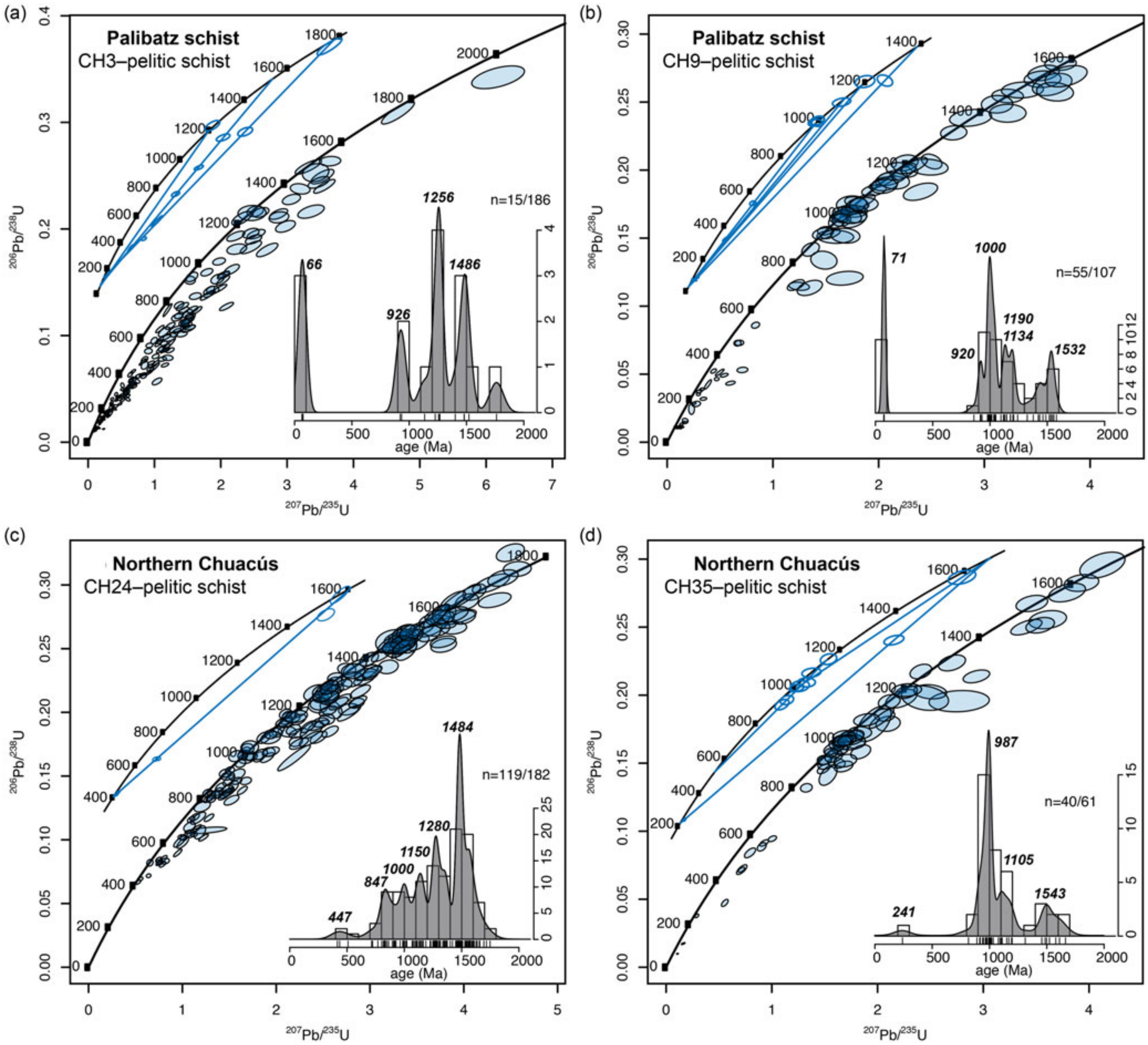

Figure 5. U-Pb zircon isotope data of metapelite samples from the Palibatz schist and northern Chuacús. (a–d) Wetherill concordia diagrams plotted with error ellipses at the 2σ level. Insets show single-grain discordia trends (blue lines) and kernel density estimates (KDEs) (Vermeesch, 2012) for data below a discordance cut-off value of 10%, where x-axis denotes single-grain concordia age in million years and y-axis shows the frequency of data. Discordance is defined as the log ratio distance to the maximum likelihood composition on the concordia line (Vermeesch, 2021).

show density peaks at ca. 1486, 1256, 926 and 66 Ma. Similar density peaks are obtained by using $^{207}Pb/^{206}Pb$ ages of the whole dataset (not shown). The apparent age of 926 Ma is taken as the maximum depositional age of the sedimentary protolith, whereas the youngest peak corresponds to metamorphic zircon overgrowths.

In sample CH9 (Pachajob), most zircon analyses (51%) are concordant or slightly discordant (≤10%), spreading along concordia between ca. 1580 and 850 Ma (Fig. 5b). The remaining discordant data indicate different discordia trends, the majority with lower intercept ages below 100 Ma. Fifty-five ages within the 10% discordance cut-off produce density peaks at ca. 1532, 1435, 1190, 1134, 1000, 920 and 71 Ma. The two youngest peaks provide the maximum depositional age of the sedimentary protolith and the age of metamorphic zircon crystallization in sample CH9, respectively.

4.a.3. Northern Chuacús metapelite

Sample CH24 (Pachirax) is a pelitic schist that consists of garnet porphyroblasts in a matrix mainly composed of phengite, paragonite, quartz, chloritoid and rutile, with minor amounts of epidote, chlorite, Fe-Ti oxide, kyanite, apatite and zircon. Most zircon grains display relatively high-CL cores with concentric, oscillatory, planar and sector zoning patterns, rimmed by darker overgrowth domains (Fig. 3). One hundred and nineteen out of 182 grains analysed are acceptable in terms of concordance (≤10%), with the majority falling along the concordia between ca. 1740 and 830 Ma (Fig. 5c). Age density peaks occur at ca. 1484, 1280, 1150, 1000 and 847 Ma. Two younger grains are concordant at ca. 509 (Th/U = 0.542) and 416 (Th/U = 0.016) Ma, but the age of ca. 847 Ma offers the more robust constraint on the maximum deposition age of the sample. Discordant grains (≥ 10%) delineate a discordia trend towards an apparent Silurian-Devonian lower intercept.

Sample CH35 (El Apazote) is a pelitic schist that contains staurolite porphyroblasts in a matrix of phengite, quartz, paragonite, garnet, chlorite, kyanite and chloritoid, plus accessory phases like rutile, apatite and zircon. Zircon crystals are analogous to those from sample CH24. Sixty-one laser spots were performed targeting both cores and rims. Core analyses mostly yielded concordant results in the 1670–799 Ma range (Fig. 5d), and 40 grains are acceptable for interpretation. Major density peaks occur at ca. 1543, 1105 and 987 Ma, with the youngest population providing the maximum depositional age of the protolith. The remaining analyses were collected on zircon rims and yielded discordant results (11–51% disc.), corresponding to different discordia trends with lower intercept ages towards the late Mesoproterozoic, early Palaeozoic and Triassic.

4.b. Zircon trace element compositions

A total of 338 points measurements were performed on zircons from all seven granitoid samples, comprising the Cubulco granitoids of ca. 1100 Ma (CH73, CH74) and 1030–1010 Ma age (CH88, CH89), the Pachajob gneiss of ca. 990 Ma age (CH10) and the Agua Caliente granitoids of ca. 225 Ma age (CH20, CH55).

Trace elements span a wide range of concentrations, both within individual samples and between them, including relevant elements in zircon like U (16–3920 μg/g), Th (3–1830 μg/g), Hf (6590–20500 μg/g) and Ti (0–78 μg/g) (Fig. 6). Most of the analysed zircons have Th/U values between 0.1 and 0.5; however, zircon from the Agua Caliente granitoids are characterized by relative high Th/U values around 1, whereas zircons from the granitoid CH89 (Cubulco unit) are typically below 0.1 (Fig. 6a). Titanium contents are highest in zircon from the Cubulco and Pachajob granitoids (up to 78 μg/g in CH74) and lowest in those from the Agua Caliente unit (up to 12 μg/g) (Fig. 6b). As a whole, the analyses show a rough positive correlation between Ti and Hf. The application of the Ti-in-zircon thermometer of Ferry and Watson (2007), assuming a value of α_{TiO2} (0.6) in the range of silicic magmas (Hayden & Watson, 2007), indicates average crystallization temperatures of 848 ± 56 °C (n = 179, 1SD), 848 ± 27 °C (n = 103, 1SD) and 741 ± 60 °C (n = 53, 1SD) for the Cubulco, Pachajob and Agua Caliente granitoids, respectively.

Zircons from the Cubulco and Pachajob samples have chondrite-normalized Eu/Eu* average values ($Eu/Eu^* = Eu_N/(Sm_N \times Gd_N)^{1/2}$) between 0.1 and 0.2, except for CH89 that show an average ratio of 0.4. By contrast, zircons from the Agua Caliente granitoids are characterized by a relatively high average Eu/Eu* value of 0.5. Similar trends are observed regarding the (Eu/Eu*)/Y × 10^4 hydration proxy of Lu *et al.* (2016), with Agua Caliente and CH89 granitoids showing the highest data density with relatively high (>1) values (Fig. 6c). On the other hand, according to the relative oxygen fugacity (ΔFMQ) values, calculated using the method of Loucks *et al.* (2020), there is a clear distinction between most of the Mesoproterozoic samples, with values mainly from −3 to 0, and the Triassic Agua Caliente granitoid that ranges

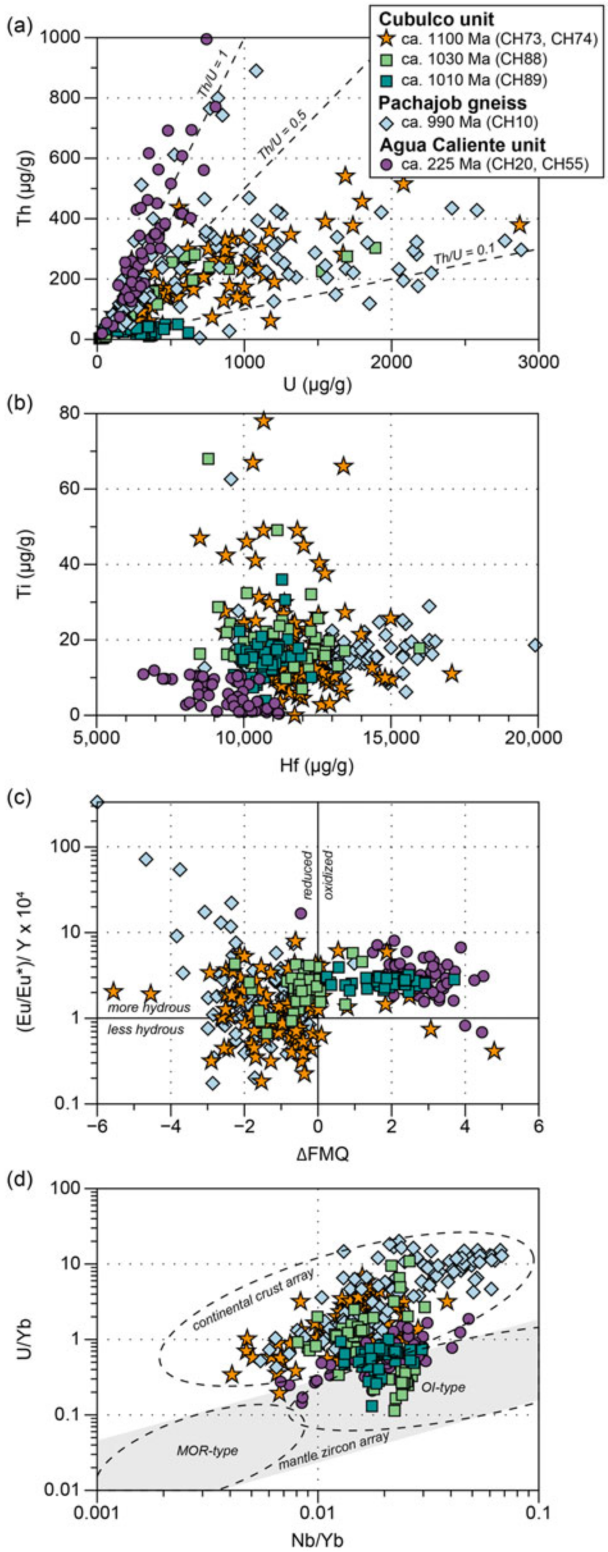

Figure 6. Zircon trace element data for metamorphosed granitoids from the Chuacús high-pressure suite. (a) Th vs. U (μg/g); dashed lines indicate Th/U values of 0.1, 0.5 and 1. (b) Ti vs. Hf (μg/g) (c) (Eu/Eu*)/Y × 10^4 vs. ΔFMQ; ΔFMQ values are calculated as 3.998 × LOG(((Ce/U) × (U/Ti))$^{0.5}$) + 2.284 (after Lu *et al.* 2016; Loucks *et al.* 2020). (d) U/Yb vs. Nb/Yb tectonic discrimination diagram (Grimes *et al.* 2015); MOR: mid-ocean ridge, OI: ocean-island.

from 1 to 5 (Fig. 6c). Again, granitoid CH89 is the exception, showing ΔFMQ values between 0 and 4.

In the U/Yb vs. Nb/Yb discrimination diagram of Grimes *et al.* (2015), most data plot in the continental crust field, but a considerable number of zircons from the Cubulco (CH88 and CH89) and Agua Caliente samples fall within the ocean-island (OI)-type mantle array.

4.c. Sm-Nd and Lu-Hf isotope systematics

Sm-Nd and Lu-Hf isotope data, including T_{DM} model ages, are presented in Table 2. Initial $^{143}Nd/^{144}Nd$ and $^{176}Hf/^{177}Hf$ ratios were recalculated at the protolith ages determined by U-Pb zircon dating (Maldonado *et al.* 2018b; this work). An age of 500 Ma was assumed for metapelite samples. The data show a positive correlation between εNd_i and εHf_i values, where granitoids conform well to the present-day Terrestrial Array (Vervoort *et al.* 2011), while metapelite samples deviate by 6 to 7 εHf units above (Fig. 7a). Granitoids have initial isotopic compositions close to CHUR, with εNd_i and εHf_i values of −1.7–0.3 and −0.3–0.8, respectively.

Figure 7b shows the Hf isotope ratios in a $^{176}Hf/^{177}Hf$ vs. time isotope evolution diagram, where samples display different evolution trends according to protolith ages. Granitoids from the Agua Caliente unit have initial Hf isotope ratios of 0.282644–0.282662 and the corresponding T_{DM} Hf model ages range from 1.04 to 1.02 Ga. The Pachajob gneiss has an initial Hf isotope ratio of 0.282159 and a T_{DM} Hf model age of 1.50 Ga. In contrast, granitoids from the Cubulco unit have initial ratios between 0.282074 and 0.282167, with relatively older T_{DM} Hf model ages between 1.73 and 1.62 Ga. Metapelites yield a narrow range of present-day Hf compositions from 0.282464 to 0.282500 and their T_{DM} Hf model ages are between 1.63–1.60 Ga (Palibatz schist) and 1.83–1.77 Ga (northern Chuacús metapelite). The Nd evolution of the samples (Fig. 7c) is quite similar to that of Hf. However, the metapelite samples have Nd isotope compositions slightly less radiogenic, decreasing up to 3ε units. Granitoid samples have initial Nd isotope ratios of 0.512281–0.512310 (Agua Caliente unit), 0.511297 (Pachajob gneiss) and 0.511217–0.511328 (Cubulco unit), with calculated T_{DM} Nd model ages of 0.93–0.88, 1.40 and 1.68–1.58 Ga, respectively. Again, metapelite samples show more restricted present-day Nd compositions ranging from 0.511900 to 0.511935, with T_{DM} Nd model ages between 1.75 and 1.54 Ga.

5. Discussion

5.a. Petrogenesis and implications of granitoid magmatism

A range of ages has previously been reported for the igneous protoliths of the Chuacús HP suite (Ratschbacher *et al.* 2009; Solari *et al.* 2011; Martens *et al.* 2012; Maldonado *et al.* 2018a, 2018b, 2023). At present, three granitoid-bearing units are clearly distinguished on the basis of age and geochemical characteristics: 1) the Cubulco unit with ca. 1100–1010 Ma granitoids, 2) the Pachajob gneiss of ca. 990 Ma and 3) the Agua Caliente unit that contains ca. 225 Ma granitoids. Although granitic rocks of Ordovician age are also recognized in the region (Solari *et al.* 2011), they are outside the presently defined limits of the HP suite and are not addressed in this section.

5.a.1. Stenian magmatism

Stenian granitoids from the Cubulco unit are mesoperthite-rich metaluminous to peraluminous and alkalic to alkalic-calcic rocks that share all the geochemical features common to A-type (ferroan) granites (Maldonado *et al.* 2018b). They show high Fe/(Fe +Mg) and K_2O/Na_2O ratios and high incompatible element contents, including Y, rare-earth elements (REE) and HFSE, which are typical for A-type granites (Collins *et al.* 1982; Whalen *et al.* 1987; Bonin, 2007; Frost & Frost, 2011). Their 10,000 × Ga/Al ratios vary from 2.8 to 3.3, within the global range of A-type granites reported by Whalen *et al.* (1987). Following the subdivision of Eby (1992), the Cubulco granitoids show an A2-type character (Y/Nb = 2.5–3.6), indicative of magma derived from a pre-existing continental crust. Trace element compositions of zircon can be used to evaluate the hydration and oxidation state as well as the tectono-magmatic source of a magma (Grimes *et al.* 2015; Lu *et al.* 2016; Loucks *et al.* 2020). Zircon trace element data for the Cubulco granitoids (Fig. 6) suggest reduced and variably hydrous crystallization conditions for the precursor magma and agree with a source in the continental crust with potential contributions from the mantle (e.g. CH88). This is true for all samples except for CH89 (ca. 1013 Ma), which suggest hydrous and oxidized conditions as well as influence from OI-type mantle material. In addition, the Ti-in-zircon thermometry suggest that the Cubulco granitoids crystallized at relatively high magmatic temperatures of 848 ± 56 °C. However, considering the ca. 100 m.y. spread in ages, this unit probably includes two granitoid groups (i.e. of ca. 1100 and 1030–1010 Ma), although no obvious petrographic or isotopic difference is observed between them.

The Cubulco unit displays a bimodal isotope distribution, where initial Nd and Hf isotope compositions of granitoids (εNd_i = −1.7–0.3, εHf_i = −0.3–0.8) are up to 10 ε units lower than those of associated eclogites (Fig. 8a) (Maldonado *et al.* 2023). These data indicate that granitoids could not have been produced by differentiation of the eclogite precursor magma, implying the existence of two distinctly different magma sources. T_{DM} model ages of the Cubulco granitoids (ca. 1.7–1.6 Ga) are significantly older (ca. 500–600 m.y.) than their crystallization ages, suggesting derivation of magma predominantly from a pre-existing less siliceous crustal source. Recycling of an older crust is also supported by inherited zircons with ages between ca. 1633 and 1235 Ma (Maldonado *et al.* 2018b). However, derivation of the precursor magmas from mafic crust alone seems unlikely, as the heat required to partially melt such a protolith would most certainly be associated with mantle upwelling (i.e. asthenospheric input). Considering the occurrence of coeval (ca. 1100–1030 Ma) metabasites (eclogites) (Maldonado *et al.* 2023), the potential contribution from isotopically juvenile magmas cannot be dismissed. It is worth noting that alkalic to alkalic-calcic A-type granitoid suites, with metaluminous or even peraluminous components, may be derived from differentiation of tholeiitic basalt magmas with variable amount of crustal contribution (Frost & Frost, 2011). Therefore, mixing between magma derived from evolved crust and mantle-derived melts could have played an important role in generating the Cubulco granitoids. Although the negative Eu anomalies (Eu/Eu*=0.5–0.7) of these granitoids, together with their apparent negative correlations of Eu/Eu* vs. SiO_2 and HFSE (Maldonado *et al.* 2018b) might indicate feldspar fractionation, additional work is needed to clarify the influence of fractional crystallization on deriving the granitic magmas. It is clear from the associated tholeiitic metabasites that this igneous suite might have involved asthenospheric melts produced either in a post-orogenic, intracontinental or back-arc setting (Collins *et al.* 2020).

Nd and Hf isotope data from the Stenian A-type granitoids in the Chuacús HP suite reflect the existence of a basement with crustal residence ages of at least 1.7–1.6 Ga. The isotopic evolution

https://doi.org/10.1017/S0016756824000347 Published online by Cambridge University Press

Table 2. Sm-Nd and Lu-Hf data for metamorphic rocks from the Chuacús high-pressure suite

Sample	Rock type	t (Ma)	Sm (μg/g)	Nd (μg/g)	$^{147}Sm/^{144}Nd$	$^{143}Nd/^{144}Nd$	± 2σ	εNd(0)	$^{143}Nd/^{144}Nd(i)$	εNd(i)	T_{DM} (Ma)
CH3	Pelitic schist	500	24.98	158.24	0.0954	0.511900	3	−14.2	0.511588	−7.8	1540
CH9	Pelitic schist	500	13.97	74.86	0.1128	0.511927	4	−13.7	0.511558	−8.4	1752
CH24	Pelitic schist	500	18.14	86.74	0.1096	0.511931	3	−13.6	0.511572	−8.1	1696
CH35	Pelitic schist	500	14.76	78.80	0.1132	0.511935	3	−13.6	0.511564	−8.3	1748
CH10	Granitoid gneiss	994	4.72	47.80	0.0597	0.511687	3	−18.4	0.511297	−1.1	1399
CH20	Granitoid gneiss	224	5.97	35.66	0.1012	0.512429	3	−3.9	0.512281	−1.2	934
CH55	Metagranite	224	5.30	32.35	0.0991	0.512455	4	−3.4	0.512310	−0.6	884
CH73	Granitoid gneiss	1101	15.48	72.36	0.1293	0.512159	3	−9.2	0.511225	0.2	1681
CH74	Metagranite	1108	11.74	65.27	0.1088	0.512008	4	−12.1	0.511217	0.2	1577
CH88	Granitoid gneiss	1026	12.98	67.18	0.1234	0.512158	4	−9.2	0.511328	0.3	1579
CH89	Granitoid gneiss	1013	11.17	71.19	0.1088	0.511964	4	−13.0	0.511241	−1.7	1638
Sample	Rock type	t (Ma)	Lu (μg/g)	Hf (μg/g)	$^{176}Lu/^{177}Hf$	$^{176}Hf/^{177}Hf$	± 2σ	εHf(0)	$^{176}Hf/^{177}Hf(i)$	εHf(i)	T_{DM} (Ma)
CH3	Pelitic schist	500	0.53	5.19	0.01456	0.282500	3	−10.1	0.282363	−3.8	1605
CH9	Pelitic schist	500	0.84	8.70	0.01377	0.282464	3	−11.4	0.282335	−4.8	1630
CH24	Pelitic schist	500	0.86	7.62	0.01610	0.282476	3	−10.9	0.282325	−5.1	1770
CH35	Pelitic schist	500	0.89	7.46	0.01701	0.282481	2	−10.8	0.282321	−5.3	1833
CH10	Granitoid gneiss	994	0.13	7.33	0.00253	0.282206	3	−20.5	0.282159	0.1	1501
CH20	Granitoid gneiss	224	0.46	5.78	0.01135	0.282692	2	−3.3	0.282644	0.0	1045
CH55	Metagranite	224	0.48	5.81	0.01178	0.282711	3	−2.6	0.282662	0.6	1024
CH73	Granitoid gneiss	1101	1.06	13.32	0.01135	0.282336	2	−15.9	0.282100	0.5	1733
CH74	Metagranite	1108	0.52	8.29	0.00895	0.282261	2	−18.5	0.282074	−0.3	1725
CH88	Granitoid gneiss	1026	0.51	7.65	0.00951	0.282340	2	−15.7	0.282156	0.7	1616
CH89	Granitoid gneiss	1013	0.49	5.29	0.01321	0.282419	3	−12.9	0.282167	0.8	1688

Initial (i) isotope ratios and ε values were recalculated according to U-Pb ages (Maldonado *et al.*, 2018a) and to assumed ages of 500 Ma for pelitic schist samples. Depleted mantle (T_{DM}) Sm-Nd model ages were calculated using present-day values of Liew and Hofmann (1988) and the $\lambda^{147}Sm$ value of Lugmair and Marti (1978). T_{DM} Lu-Hf model ages were calculated using present-day values of Vervoort *et al.* (2000) and the $\lambda^{176}Lu$ value of Scherer *et al.* (2001) and Söderlund *et al.* (2004). εNd and εHf values were calculated using chondritic uniform reservoir (CHUR) values after Bouvier *et al.* (2008).

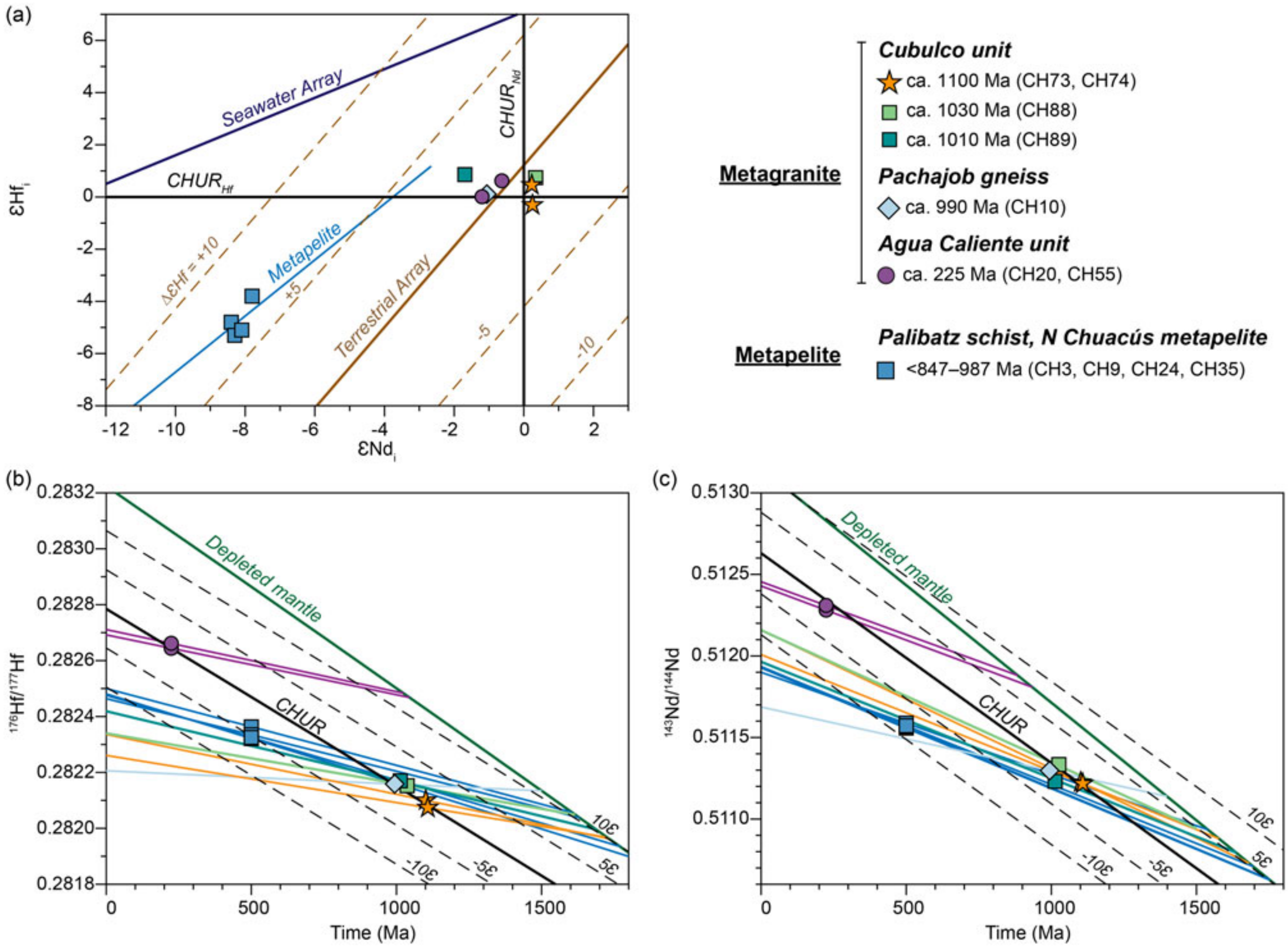

Figure 7. Sm-Nd and Lu-Hf isotope data of whole-rock samples from the Chuacús high-pressure suite. (a) Initial εHf vs. εNd recalculated to estimated protolith ages shown in Table 2. εNd and εHf values are plotted with respect to the chondritic uniform reservoir (CHUR), using the data of Bouvier (2008). The present-day Terrestrial Array, calculated as εHf = 1.55εNd + 1.21 (Vervoort *et al.* 2011), is shown together with lines of constant deviation of Hf (ΔεHf) from this expression. The Seawater Array is as follows: εHf = 0.55εNd + 7.1 (Albarède *et al.* 1998). The Metapelite line corresponds to a regression through the isotope compositions calculated at ages younger than the estimated maximum depositional ages. (b) $^{176}Hf/^{177}Hf$ vs. time diagram showing the isotopic evolution of the samples. The Depleted Mantle line is after Vervoort *et al.* (2000). Dotted lines are deviations in +5 and −5 εHf increments from CHUR. (c) $^{143}Nd/^{144}Nd$ vs. time diagram showing the isotopic evolution of the samples. The Depleted Mantle line is after Liew & Hofmann (1988). Analogous to the Hf plot, dotted lines are deviations in +5 and −5 εNd increments from CHUR.

trends of these rocks, in general, coincide with those of the eclogites from the El Chol unit (Maldonado *et al.* 2023) (Fig. 8a). Even though the apparently Ectasian (ca. 1310 Ma) age of the El Chol mafic protoliths must still be confirmed, their isotopic similarity to the A-type Cubulco granitoids would indicate a genetic relationship between both units. Moreover, the ca. 1630 Ma zircon inheritance in the Cubulco granitoids (Maldonado *et al.* 2018a) suggests the recycling of late Palaeoproterozoic crust that might be similar to the Calymmian basement recently discovered in the nearby Chiapas Massif (Valencia-Morales *et al.* 2022). The Nd evolution is also in the range of the late Mesoproterozoic basement of Mexico (e.g. Oaxaquia; Fig. 8a), and some notable similarities also exist between the Cubulco granitoids and contemporaneous rocks from the cordilleran inliers of Colombia, particularly the Guapotón gneiss in the Garzón Massif (Ibanez-Mejia *et al.* 2015). A review of potential correlations between the Cubulco unit and areas recording Stenian bimodal (LIP-related) magmatism across Amazonia, Baltica and Laurentia was recently presented in Maldonado *et al.* (2023). One important additional observation is that most of the Stenian A-type plutonism around Rodinia is associated with rift-hotspot activity within Laurentia (Condie *et al.* 2023). An exception to this is the Sunsás belt of Bolivia (Amazonia), were hybrid A-type granitoids were produced during post-collisional magmatism at ca. 1.1 Ga (Nedel *et al.* 2020).

5.a.2. Tonian magmatism

The Pachajob gneiss, with protolith ages of ca. 990 Ma, consists of a high-silica, peraluminous and alkalic-calcic granitoid, interpreted by Maldonado *et al.* (2018b) as a crustal partial melt. These authors also reported a highly fractionated REE pattern with concave heavy REE profile as well as negative Ta, Nb, Sm and Ti anomalies, which probably indicate a source in a middle-lower crust with residual amphibole/clinopyroxene and rutile. Zircon trace element data presented in this work (Fig. 6) are consistent with a magma of crustal origin that crystallized under reduced and variably hydrous conditions (see discussion above).

Just as for the Cubulco granitoids, the crystallization age of the Pachajob gneiss is significantly younger (ca. 400–500 m.y.) than the T_{DM} model ages (Fig. 7). However, the Nd and Hf isotope evolution trends are less steep for the Pachajob gneiss and yield comparatively younger T_{DM} model ages (1.5–1.4 Ga), indicating derivation from melting of rejuvenated crust. Figure 8a shows that

https://doi.org/10.1017/S0016756824000347 Published online by Cambridge University Press

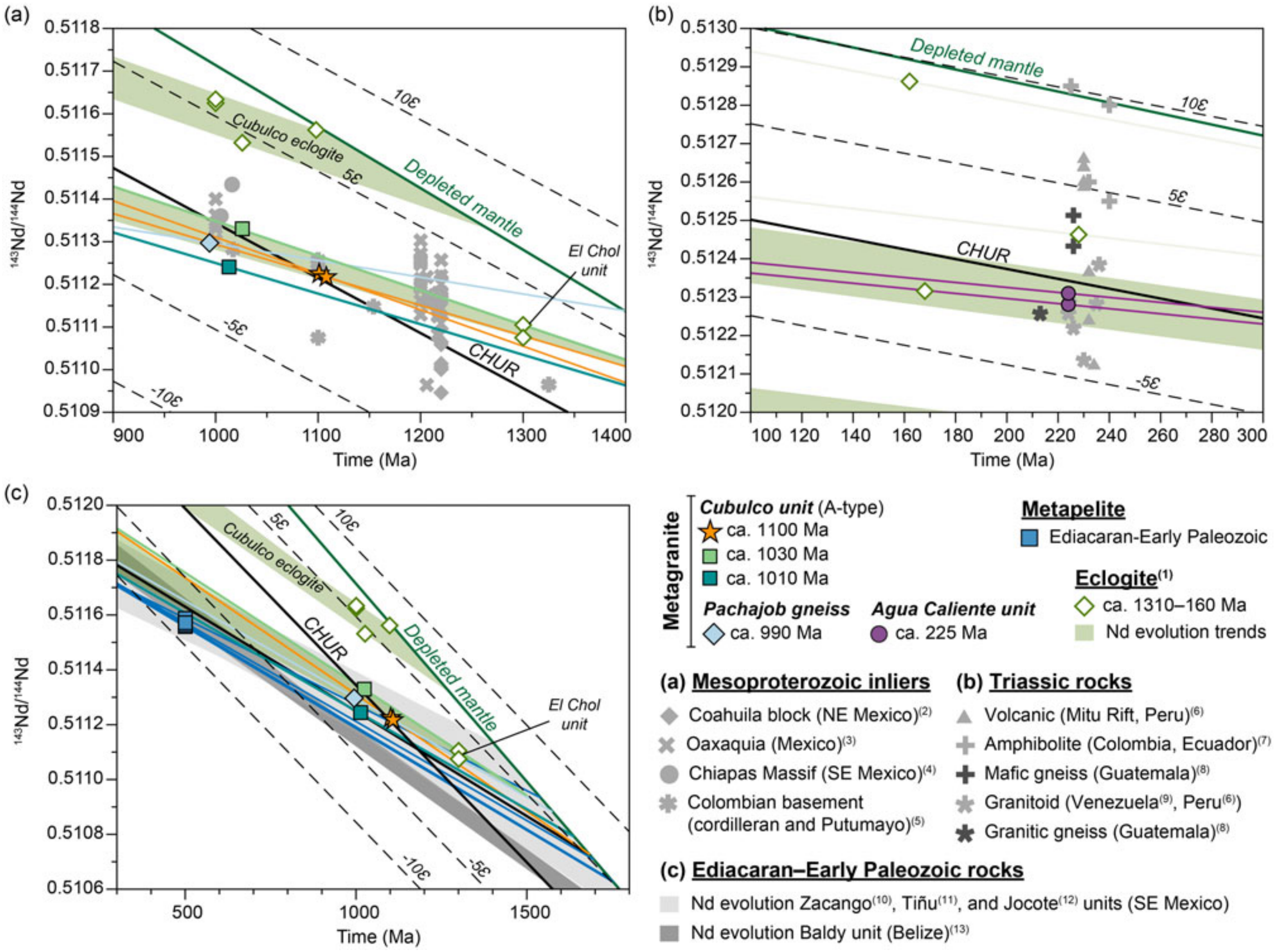

Figure 8. $^{143}Nd/^{144}Nd$ vs. time plots showing the isotopic evolution of whole rocks from the Chuacús high-pressure suite together with reference data used for comparison, as discussed in the text. The parameters and nomenclature are the same as in Figure 7. Whole-rock reference data is from (1) Maldonado *et al.* (2023); (2) Lopez *et al.* (2001); (3) Patchett and Ruiz (1987), Ruiz *et al.* (1988), Weber and Köhler (1999), Weber *et al.* (2010); (4) Weber *et al.* (2018); (5) Restrepo-Pace *et al.* (1997), Ibanez-Mejia (2015); (6) Spikings *et al.* (2016); (7) Cochrane *et al.* (2014); (8) Solari *et al.* (2011); (9) Tazzo-Rangel *et al.* (2019); (10) Ortega-Obregon *et al.* (2010); (11) Murphy *et al.* (2005); (12) González-Guzmán *et al.* (2016); (13) Weber *et al.* (2012).

model ages for the Pachajob gneiss fall between those from the Cubulco unit (granitoids and eclogites). Accordingly, taking into account the protolith age and zircon inheritance (ca. 1200–1120 Ma) of the Pachajob gneiss (Maldonado *et al.* 2018b), we interpret that the magma was sourced from a crust similar in age and composition to the Cubulco unit. The Ti-in-zircon thermometer suggests a relatively high crystallization temperature of the magma of 848 ± 27 °C. Therefore, considering that mafic (tholeiitic) magmatism within the currently adjacent Cubulco unit probably spans the Stenian-Tonian boundary (Maldonado *et al.* 2023), it is plausible that the associated heat transfer induced partial melting of the latest Mesoproterozoic middle-lower crust. Even if this interpretation is valid, whether the Pachajob and the youngest Cubulco (1030–1010 Ma) granitoids would represent a single long-lived episode of extensional magmatism or two separated episodes remains to be demonstrated.

Initial Nd ratios of the Pachajob gneiss are slightly less radiogenic but overall comparable with those of AMCG (anorthosite-mangerite-charnockite-granite) suite rocks from Oaxaquia and granitic orthogneiss from the Chiapas Massif (Weber & Köhler, 1999; Weber *et al.* 2018) (Fig. 8a). An alternative correlation for the early Tonian anatexis recorded by the Pachajob gneiss is the late Mesoproterozoic (ca. 1.05–1.02 Ga) migmatization identified in both the Cordilleran inliers and the Putumayo Basin basement of Colombia (Cordani *et al.* 2005; Ibanez-Mejia *et al.* 2011; Ibanez-Mejia *et al.* 2015), which has been interpreted as related to accretionary tectonics.

5.a.3. Late Triassic magmatism

Late Triassic megacrystic granitoids within the Agua Caliente unit are metaluminous to peraluminous and alkalic-calcic, showing enrichment in light REE and flat heavy REE profiles, negligible or absent Sr and Eu anomalies and relatively high HFSE concentrations (Solari *et al.* 2011; Maldonado *et al.* 2018b). These features reflect negligible fractional crystallization of a magma that incorporate an enriched component. On the other hand, U/Yb vs. Nb/Yb covariation in zircon (Grimes *et al.* 2015) (Fig. 6d) suggests a magma formed by mixing of continental crust and enriched mantle material. Coeval tholeiitic metabasites (eclogites) were interpreted by Maldonado *et al.* (2023) as produced from an enriched sub-lithospheric mantle during a pulse of intraplate continental magmatism. The initial isotope compositions of the Agua Caliente granitoids ($\varepsilon Nd_i = -1.1, -0.6, \varepsilon Hf_i = 0, 0.6$) are up to 4 ε units below the values of associated eclogite (Fig. 8b). As T_{DM}

https://doi.org/10.1017/S0016756824000347 Published online by Cambridge University Press

model ages (ca. 1.0–0.9 Ga) for the granitoids are significantly older than the ages of crystallization (ca. 225 Ma), the magmas must have incorporated an important volume of older crustal material. This interpretation is supported by Stenian-Tonian (ca. 1050–980 Ma) zircon inheritance within these rocks (Maldonado *et al.* 2018b). Accordingly, an explanation that likely accounts for the origin of the Agua Caliente granitoids envisages a magma derived largely from older (late Mesoproterozoic) continental crust (e.g. Cubulco unit), with additional contributions from enriched mantle material. Thermal maturation and collapse of a thickened orogenic crust may result in extensive hybridization of partial melts derived from a heterogeneous lower crust and enriched mantle (Jacob *et al.* 2021). A post-collisional setting, rather than an intraplate one, would be more consistent with oxidized and relatively hydrous crystallization conditions, as suggested by zircon trace element compositions (Fig. 6c). Although magmatic temperatures for the Agua Caliente granitoids, estimated at 741 ± 60 °C, are lower than would be expected in a post-collisional setting (Sylvester, 1998), the paucity of inherited zircon would indicate that melting temperatures were above zircon saturation and eventually sufficient to melt a fertile crust (e.g. Gerdes *et al.* 2000).

As discussed previously in Maldonado *et al.* (2018a, 2023), the Agua Caliente unit is mostly correlative with regions representing a western Pangea rift system during the Late Triassic in what is today western and northern South America. Figure 8b shows that granitoids from the Agua Caliente unit have initial Nd isotope ratios in the range of Nd compositions of silicic rocks from the Venezuelan and Peruvian Andes (Spikings *et al.* 2016; Tazzo-Rangel *et al.* 2019). However, the mafic components are considerably less radiogenic than metabasite and mafic volcanics of that region (Cochrane *et al.* 2014). Whether the Agua Caliente unit included Triassic magmas sourced from a depleted mantle, either pristine or later modified by contamination, is still an unsolved subject that goes beyond the scope of this paper.

5.b. Palaeozoic and Mesozoic sedimentary record

The Chuacús HP suite contains abundant metasedimentary rocks, including pelitic schist, quartzite, marble and calc-silicate rocks. The youngest detrital zircon populations in the Palibatz schist (southern Sierra de Chuacús) occur at ca. 920 and 670 Ma (Solari *et al.* 2011, this work), indicating a post-Cryogenian depositional age of its protolith. The minimum age of deposition is constrained by Lu-Hf ages of ca. 100 Ma, obtained from metamorphic garnet (Maldonado *et al.* 2018a). The isotopic compositions of the Palibatz schist deviate more than 4 εHf units above the Terrestrial Array (Fig. 7a), reflecting a zircon deficit that is typical of terrigenous clays dominated by continental sources (Albarède *et al.* 1998; Vervoort *et al.* 2011). Although Hf isotopic signatures in marine sediments are controlled by Lu/Hf fractionation during weathering, transport and diagenesis, the Nd composition is basically unaffected by these processes, reflecting the signature of the source regions (Vervoort *et al.* 2011). Therefore, the Sm-Nd systematics can be used to trace the provenance of the Palibatz schist. T_{DM} Nd model ages of 1.8 and 1.5 Ga express the integrated age of all crustal components in this unit. These ages are in the range of T_{DM} Nd model ages of the Cubulco granitoids and the El Chol unit (Fig. 8c) and also coincide with those reported for the basement exposures of Oaxaquia and the Colombian Andes (Ruiz *et al.* 1988); Weber & Köhler, 1999; Lopez *et al.* 2001); Ibanez-Mejia *et al.* 2015), suggesting that most of the detritus could have been derived from Mesoproterozoic crust. The Palibatz schist is characterized by major detrital zircon peaks at ca. 1.5, 1.2 and 1.0 Ga. Potential sources of these zircon components may be igneous and metamorphic rocks within Oaxaquia and the Chiapas Massif (Solari *et al.* 2003; Weber *et al.* 2010; Weber *et al.* 2018; Valencia-Morales *et al.* 2022), the Cordilleran-Putumayo basement (Cuadros *et al.* 2014; Ibanez-Mejia *et al.* 2015) and the Amazonian craton (Bettencourt *et al.* 1999; Teixeira *et al.* 2010). On the other hand, these age spectra are also characteristic of pre-Ordovician (meta)sedimentary sequences across the Maya block and surrounding areas in Mexico. For instance, early Palaeozoic rocks of the Acatlán and El Triunfo complexes of southern Mexico (Talavera-Mendoza *et al.* 2005; Weber *et al.* 2008; Ramos-Arias & Keppie, 2011; González-Guzmán *et al.* 2016), the San Gabriel unit of central Guatemala (Solari *et al.* 2009) and the Baldy unit of Belize (Martens *et al.* 2010) contain distinctive Stenian (1.2–1.0 Ga) and Calymmian (ca. 1.5 Ga) zircon populations. Given the conspicuous absence of early Palaeozoic zircon in the Palibatz schist and the overall similarity to pre-Ordovician sequences in the region, we interpret that the protolith of this unit was deposited between the Ediacaran and the early Palaeozoic. This interpretation is in agreement with the occurrence of HP calc-silicate rocks with protolith ages constrained between ca. 1020 and 420 Ma (Maldonado *et al.* 2023). Figure 8c shows that the Nd evolution trends of the Palibatz samples are in the range of those of the Zacango (Acatlán Complex), Jocote (Triunfo Complex) and Tiñu units of southern Mexico (Murphy *et al.* 2005; Ortega-Obregón *et al.*, 2010; González-Guzmán *et al.* 2016), whereas they clearly diverge from the Baldy unit (Weber *et al.* 2012). Considering lithology, U-Pb ages and Sm-Nd isotopes, we note striking similarities with both the Jocote (Ediacaran) and Tiñu (Early Ordovician) units.

In addition to the late Neoproterozoic–early Palaeozoic sedimentary sequence, U-Pb ages of detrital zircon from different areas within the Chuacús HP suite suggest the existence of late Palaeozoic and post-Triassic strata (Ratschbacher *et al.* 2009; Solari *et al.* 2009; Solari *et al.* 2011; Martens *et al.* 2012). Evidence for late Palaeozoic sedimentation comes from a single sample from northern Sierra de Chuacús, containing early Palaeozoic (480–402 Ma) detrital zircon (Solari *et al.* 2009). Unfortunately, additional evidence on the precise timing of this sedimentation period is currently lacking. In the Maya block, and several other areas of southern and eastern Mexico, early Palaeozoic rocks are overlain by clastic Carboniferous–Permian sequences (e.g. Santa Rosa Group) that typically contain Early Ordovician–Silurian detrital zircon (Weber *et al.* 2009; Martens *et al.* 2010; Guerrero-Moreno *et al.* 2023). Interestingly, our samples from northern Sierra de Chuacús (CH24, CH35), which belong to the structurally lower levels where HP features are visible, do not provide further evidence for this probable late Palaeozoic sequence. Both samples lack zircon populations spanning Ordovician to Silurian periods but have major components of Calymmian–Ectasian (1.5–1.2 Ga) zircon (Figs. 5c, d). Although some zircons yield early Palaeozoic or even younger (slightly discordant) ages, the evidence is not conclusive, and the rocks are ultimately more comparable to the Palibatz schist.

Post-Triassic sedimentation is inferred from eclogitic paragneisses showing a detrital zircon population spanning 280–220 Ma (Solari *et al.* 2011; Martens *et al.* 2012). Based on their mineralogy which includes quartz, white mica, omphacite, garnet and rutile, we suggest that these rocks were probably derived from mixed quartzose and mafic volcanic sediments. Maldonado *et al.* (2023)

reported Middle Jurassic (170–160 Ma) eclogite protoliths that likely formed from mafic volcaniclastic deposits with E-MORB affinity. We interpret that deposition of mixed sediments might have been simultaneous and closely related to Middle Jurassic E-MORB-like magmatism, in response to continental rift basin development around the proto-Gulf of Mexico. This record may potentially be correlated with several Middle Jurassic volcaniclastic sequences (mostly acid to intermediate) exposed from northern Mexico to Chiapas (Godínez-Urban *et al.* 2011; Rubio-Cisneros & Lawton, 2011), presently grouped into the Nazas rift province (Busby & Centeno-García, 2022).

6. Concluding remarks

Three periods of granitic magmatism at ca. 1100–1010, 990 and 225 Ma are recognized in the Chuacús HP suite. Stenian A-type granitoids within the bimodal Cubulco unit formed through mixing of magmas derived from late Palaeoproterozoic crust and mantle-derived melts produced either in a post-orogenic, intra-continental or back-arc setting within assembling Rodinia. Whether the Cubulco granitoids represent a protracted and continuous period (ca. 100 m.y.), or two separate pulses (1100 and 1030–1010 Ma) of magmatism remains an open question. The precursor magma of Tonian granitoids (Pachajob gneiss) was generated by partial melting of rejuvenated late Mesoproterozoic middle-lower crust associated with extensional tectonics. Late Triassic granitoids of the bimodal Agua Caliente unit were probably formed by mixing between melts derived from late Mesoproterozoic crust and melts derived from an enriched mantle in a post-collisional setting that evolved into continental rifting. This extensional stage, related to the western Pangea breakup, would have led to considerable thinning of the Chuacús crust and its consolidation as a passive margin that eventually subducted in the Cretaceous.

Even though the Chuacús HP suite may include late Palaeozoic and Jurassic metasedimentary rocks, most of the protoliths were probably deposited between the Ediacaran and the early Palaeozoic. The most characteristic unit is the Palibatz schist, which consists mainly of metapelite formed from terrigenous clays sourced from Mesoproterozoic continental areas such as the Chuacús basement itself or the basement inliers of southern Mexico and the northern Andes. This unit may correlate with peri-Gondwanan, Ediacaran to Cambro-Ordovician sequences of southern Mexico. The metapelite sequence from the northern Sierra de Chuacús does not provide further evidence for younger sedimentation periods, but rather correlates with the Palibatz schist.

Supplementary material. The supplementary material for this article can be found at https://doi.org/10.1017/S0016756824000347

Acknowledgments. This work was supported by the PAPIIT-DGAPA-UNAM project IA102523 and a DGAPA-UNAM-postdoctoral fellowship, both granted to R. Maldonado. We want to acknowledge P. Schaaf and B. Weber for providing analytical support and for discussions about the isotopic data. We also thank S. Morán-Ical for helping in the fieldwork. C. Ortega-Obregón, C. Macías-Romo, S. Padilla-Ramírez, G. Fernández-Catá, L. Luna, G. Arrieta-García and G. Solís-Pichardo are thanked for their technical assistance during the analytical procedures. Åke Johansson, Chunjing Wei and an anonymous referee provided very constructive review of the manuscript.

Competing interests. The authors declare none

References

Albarède F, Simonetti A, Vervoort JD, Blichert-Toft J and Abouchami W (1998) A Hf-Nd isotopic correlation in ferromanganese nodules. *Geophysical Research Letters* **25**(20), 3895–98.

Anderson T.H., Burkart B, Clemons RE, Bohnenberger OH and Blount DN (1973) Geology of the western altos Cuchumatanes, Northwestern Guatemala. *GSA Bulletin* **84**(3), 805–26.

Authemayou C, Brocard G, Teyssier C, Simon-Labric T, Guttiérrez A, Chiquín EN and Morán S (2011) The Caribbean–North America–Cocos triple junction and the dynamics of the Polochic–Motagua fault systems: pull-up and zipper models. *Tectonics* **30**, TC3010.

Beccaluva L (1995) The northwestern border of the Caribbean Plate in Guatemala: new geological and petrological data on the Motagua ophiolitic belt. *Ofioliti* **20**, 1–15.

Bettencourt JS, Tosdal RM, Leite WB and Payolla BL (1999) Mesoproterozoic rapakivi granites of the Rondônia Tin Province, southwestern border of the Amazonian craton, Brazil - I. Reconnaissance U–Pb geochronology and regional implications. *Precambrian Research* **95**(1), 41–67.

Bonin B (2007) A-type granites and related rocks: Evolution of a concept, problems and prospects. *Lithos* **97**(1), 1–29.

Bouvier A, Vervoort JD and Patchett PJ (2008) The Lu–Hf and Sm–Nd isotopic composition of CHUR: Constraints from unequilibrated chondrites and implications for the bulk composition of terrestrial planets. *Earth and Planetary Science Letters* **273**(1), 48–57.

Brueckner HK, Avé lallemant HG, Sisson VB, Harlow GE, Hemming SR, Martens U, Tsujimori T and Sorensen SS (2009) Metamorphic reworking of a high pressure–low temperature mélange along the motagua fault, Guatemala: a record of Neocomian and Maastrichtian transpressional tectonics. *Earth and Planetary Science Letters* **284**(1), 228–35.

Busby CJ and Centeno-garcía E (2022) The "Nazas Arc" is a continental rift province: implications for Mesozoic tectonic reconstructions of the southwest Cordillera, U.S. and Mexico. *Geosphere* **18**(2), 647–69.

Cochrane R, Spikings R, Gerdes A, Ulianov A, Mora A, Villagómez D, Putlitz B and Chiaradia M (2014) Permo-Triassic anatexis, continental rifting and the disassembly of western Pangaea. *Lithos* **190–191**, 383–402.

Collins WJ, Beams SD, White, AJR and Chappell BW (1982) Nature and origin of A-type granites with particular reference to southeastern Australia. *Contributions to Mineralogy and Petrology* **80**(2), 189–200.

Collins WJ, Huang H-Q, Bowden P and Kemp AIS (2020) Repeated S–I–A-type granite trilogy in the Lachlan Orogen and geochemical contrasts with A-type granites in Nigeria: implications for petrogenesis and tectonic discrimination. *Geological Society, London, Special Publications* **491**(1), 53–76.

Condie KC, Pisarevsky SA, Puetz SJ, Roberts NMW. and Spencer CJ (2023) A-type granites in space and time: relationship to the supercontinent cycle and mantle events. *Earth and Planetary Science Letters* **610**, 118125.

Cordani UG, Cardona A, Jimenez DM, Liu D and Nutman AP (2005) Geochronology of Proterozoic basement inliers in the Colombian Andes: tectonic history of remnants of a fragmented Grenville belt. *Geological Society, London, Special Publications* **246**(1), 329–46.

Cuadros FA, Botelho NF, Ordóñez-carmona O and Matteini M (2014) Mesoproterozoic crust in the San Lucas Range (Colombia): an insight into the crustal evolution of the northern Andes. *Precambrian Research* **245**, 186–206.

Dengo G (1969) Problems of tectonic relations between Central America and the Caribbean. *Gulf Coast Association of Geological Societies Transactions* **19**, 311–20.

Donnelly TW, Home GS, Finch RC and López-Ramos E (1991) Northern Central America; The maya and Chortis blockse. In *The Caribbean Region* (eds. G. Dengo and J. E. Case), Geological Society of America.

Draper G, Gutiérrez G and Lewis JF (1996) Thrust emplacement of the Hispaniola peridotite belt: orogenic expression of the mid-Cretaceous Caribbean arc polarity reversal? *Geology* **24**(12), 1143–46.

Eby GN (1992) Chemical subdivision of the A-type granitoids:petrogenetic and tectonic implications. *Geology* **20**(7), 641–44.

Ferry JM and Watson EB (2007) New thermodynamic models and revised calibrations for the Ti-in-zircon and Zr-in-rutile thermometers. *Contributions to Mineralogy and Petrology* **154**(4), 429–37.

Flores KE, Martens UC, Harlow GE, Brueckner HK and Pearson NJ (2013) Jadeitite formed during subduction: In situ zircon geochronology constraints from two different tectonic events within the Guatemala Suture Zone. *Earth and Planetary Science Letters* **371–372**, 67–81.

Frost CD and Frost BR (2011) On Ferroan (A-type) Granitoids: their compositional variability and modes of origin. *Journal of Petrology* **52**(1), 39–53.

García-Casco A, Torres-Roldán RL, Iturralde-Vinent MA, Millán G, Nuñez-Cambra K, Lázaro C and Rodríguez-Vega A (2006) High pressure metamorphism of ophiolites in Cuba. *Geologica Acta* **4**(1–2), 63–88.

Gerdes A., Wörner, G. and Henk, A. (2000) Post-collisional granite generation and HT–LP metamorphism by radiogenic heating: the Variscan South Bohemian Batholith. *Journal of the Geological Society* **157**(3), 577–87.

Giunta G, Beccaluva L, Coltorti M, Mortellaro D, Siena F and Cutrupia D (2002) The peri-Caribbean ophiolites: structure, tectono-magmatic significance and geodynamic implications. *Caribbean Journal of Earth Science* **36**, 1–20.

Godínez-Urban A, Lawton TF, Molina Garza RS, Iriondo A, Weber B and López-Martínez M (2011) Jurassic volcanic and sedimentary rocks of the la silla and todos santos formations, chiapas: record of nazas arc magmatism and rift-basin formation prior to opening of the Gulf of Mexico. *Geosphere* **7**(1), 121–44.

González-Guzmán R., Weber B, Manjarrez-Juárez R, Cisneros De León A, Hecht L and Herguera-García JC (2016) Provenance, age constraints and metamorphism of Ediacaran metasedimentary rocks from the El Triunfo complex (SE Chiapas, México): evidence for Rodinia breakup and Iapetus active margin. *International Geology Review* **58**(16), 2065–91.

Grimes CB, Wooden JL, Cheadle MJ and John BE (2015) "Fingerprinting" tectono-magmatic provenance using trace elements in igneous zircon. *Contributions to Mineralogy and Petrology* **170**(5), 46.

Guerrero-Moreno S, Solari LA, Ortega-Flores B, Maldonado R and Ortega-Obregón C (2023) Provenance of Carboniferous-Permian sedimentary units in southern Mexico: evidence for peri-arc basin evolution during the Pangea assembly. *International Geology Review* **65**(20), 3100–3127.

Harlow GE., Hemming SR, Lallemant HGA, Sisson VB and Sorensen SS (2004). Two high-pressure–low-temperature serpentinite-matrix mélange belts, Motagua fault zone, Guatemala: a record of Aptian and Maastrichtian collisions. *Geology* **32**(1), 17–20.

Hayden LA and Watson EB (2007) Rutile saturation in hydrous siliceous melts and its bearing on Ti-thermometry of quartz and zircon. *Earth and Planetary Science Letters* **258**(3), 561–68.

Ibanez-Mejia M, Ruiz J, Valencia VA, Cardona A, Gehrels GE and Mora AR (2011) The putumayo orogen of amazonia and its implications for rodinia reconstructions: New U–Pb geochronological insights into the Proterozoic tectonic evolution of northwestern South America. *Precambrian Research* **191**(1), 58–77.

Ibanez-Mejia M, Pullen A, Arenstein J, Gehrels GE, Valley J, Ducea MN, Mora AR, Pecha M and Ruiz, J. (2015) Unraveling crustal growth and reworking processes in complex zircons from orogenic lower-crust: The Proterozoic putumayo orogen of Amazonia. *Precambrian Research* **267**, 285–310.

Jacob J-B, Moyen J-F, Fiannacca P, Laurent O, Bachmann O, Janoušek V, Farina F and Villaros A (2021) Crustal melting vs. fractionation of basaltic magmas: Part 2, Attempting to quantify mantle and crustal contributions in granitoids. *Lithos* **402–403**, 106292.

Kesler SE, Josey WL and Collins EM (1970) Basement rocks of Western Nuclear Central America: The Western Chuacús Group, Guatemala. *GSA Bulletin* **81**(11), 3307–22.

Liew TC and Hofmann AW (1988) Precambrian crustal components, plutonic associations, plate environment of the hercynian fold belt of central Europe: Indications from a Nd and Sr isotopic study. *Contributions to Mineralogy and Petrology* **98**(2), 129–38.

Lopez R, Cameron KL and Jones NW (2001) Evidence for Paleoproterozoic, Grenvillian, and Pan-African age Gondwanan crust beneath northeastern Mexico. *Precambrian Research* **107**(3), 195–214.

Loucks RR, Fiorentini ML and Henríquez GJ (2020) New magmatic oxybarometer using trace elements in zircon. *Journal of Petrology* **61**(3), egaa034.

Lu Y-J, Loucks RR, Fiorentini M, Mccuaig TC, Evans NJ, Yang Z-M, Hou Z-Q, Kirkland CL, Parra-Avila LA and Kobussen A (2016) Zircon compositions as a pathfinder for Porphyry Cu ± Mo ± Au deposits.

Lugmair GW and Marti K (1978) Lunar initial 143Nd/144Nd: Differential evolution of the lunar crust and mantle. *Earth and Planetary Science Letters* **39**(3), 349–57.

Maldonado R, Ortega-Gutiérrez F and Hernández-Uribe D (2016) Garnet–chloritoid–paragonite metapelite from the Chuacús Complex (Central Guatemala): new evidence for continental subduction in the North America–Caribbean plate boundary. *European Journal of Mineralogy* **28**(6), 1169–86.

Maldonado R, Weber B, Ortega-Gutiérrez F and Solari LA (2018a) High-pressure metamorphic evolution of eclogite and associated metapelite from the Chuacús complex (Guatemala Suture Zone): constraints from phase equilibria modelling coupled with Lu-Hf and U-Pb geochronology. *Journal of Metamorphic Geology* **36**(1), 95–124.

Maldonado R, Ortega-Gutiérrez F and Ortíz-Joya GA (2018b) Subduction of Proterozoic to Late Triassic continental basement in the Guatemala suture zone: A petrological and geochronological study of high-pressure metagranitoids from the Chuacús complex. *Lithos* **308–309**(2018), 83–103.

Maldonado R., Solari L, Schaaf P and Weber B (2023) A Mesoproterozoic to Jurassic history of continental eclogites from the Guatemala Suture Zone–implications for a peri-Amazonian ancestry. *Gondwana Research* **119**, 262–81.

Maresch W.V., Kluge R, Baumann A, Pindell JL, Krückhans-Lueder G and Stanek, K. (2009) The occurrence and timing of high-pressure metamorphism on Margarita Island, Venezuela: a constraint on Caribbean-South America interaction. *Geological Society, London, Special Publications* **328**(1), 705–41.

Martens U, Weber B and Valencia VA (2010) U/Pb geochronology of Devonian and older Paleozoic beds in the southeastern Maya block, Central America: Its affinity with peri-Gondwanan terranes. *GSA Bulletin* **122**(5–6), 815–29.

Martens U, Tsujimori T and Liou JG (2017) Eclogite varieties and petrotectonic evolution of the northern Guatemala suture complex. *International Geology Review* **59**(5–6), 721–40.

Martens UC, Brueckner HK, Mattinson CG, Liou JG and Wooden JL (2012) Timing of eclogite-facies metamorphism of the Chuacús complex, Central Guatemala: Record of Late Cretaceous continental subduction of North America's sialic basement. *Lithos* **146–147**, 1–10.

Murphy JB, Keppie JD, Braid JF and Nance RD (2005) Geochemistry of the Tremadocian Tiñu Formation (Southern Mexico): provenance in the underlying ~1 Ga Oaxacan complex on the Southern Margin of the Rheic Ocean. *International Geology Review* **47**(9), 887–900.

Nedel IM, Fuck RA, Ruiz AS, Matos R and Ferreira ACD (2020) U–Pb geochronology and geochemistry of grenville-age plutons in the sunsas belt - Bolivia, SW Amazonian Craton: Tectonic and magmatic implications. *Journal of South American Earth Sciences* **104**, 102845.

O'Brien PJ (2019) Eclogites and other high-pressure rocks in the Himalaya: a review. *Geological Society, London, Special Publications* **483**(1), 183–213.

Obrist-Farner J, Eckert A, Locmelis M, Crowley JL, Mota-Vidaure B, Lodolo E, Rosenfeld J and Duarte E (2020) The role of the Polochic Fault as part of the North American and Caribbean Plate boundary: insights from the infill of the Lake Izabal Basin. *Basin Research* **32**(6), 1347–64.

Ortega-Gutiérrez F, Solari LA, Ortega-Obregón C, Elías-Herrera M, Martens U, Morán-Icál S, Chiquín M, Keppie JD, De León RT and Schaaf P (2004) Polyphase, high-temperature Eclogite-Facies metamorphism in the Chuacús Complex, Central Guatemala: petrology, geochronology, and tectonic implications. *International Geology Review* **46**(5), 445–70.

Ortega-Gutiérrez F, Solari LA, Ortega-Obregón C, Elías-Herrera M, Martens U, Morán-Icál S, Chiquín M, Keppie JD, De León RT and Schaaf P (2007) The maya-Chortís boundary: a tectonostratigraphic approach. *International Geology Review* **49**(11), 996–1024.

Ortega-Obregón C, Solari LA, Keppie JD, Ortega-Gutiérrez F, Solé J and Morán-Icál S (2008) Middle-Late Ordovician magmatism and Late Cretaceous collision in the southern maya block, Rabinal-Salamá area, central Guatemala: implications for North America–Caribbean plate tectonics. *GSA Bulletin* **120**(5–6), 556–70.

Ortega-Obregón C, Murphy JB and Keppie JD (2010) Geochemistry and Sm–Nd isotopic systematics of Ediacaran–Ordovician, sedimentary and bimodal igneous rocks in the western Acatlán Complex, southern Mexico: Evidence for rifting on the southern margin of the Rheic Ocean. *Lithos* **114**(1), 155–67.

Patchett PJ and Ruiz J (1987) Nd isotopic ages of crust formation and metamorphism in the Precambrian of eastern and southern Mexico. *Contributions to Mineralogy and Petrology* **96**(4), 523–28.

Pindell J, Maresch WV, Martens U and Stanek K (2012) The Greater Antillean Arc: Early Cretaceous origin and proposed relationship to Central American subduction mélanges: implications for models of Caribbean evolution. *International Geology Review* **54**(2), 131–43.

Ramos-Arias MA and Keppie JD (2011) U–Pb Neoproterozoic–Ordovician protolith age constraints for high- to medium-pressure rocks thrust over low-grade metamorphic rocks in the Ixcamilpa area, Acatlán Complex, southern Mexico. *Canadian Journal of Earth Sciences* **48**(1), 45–61.

Ratschbacher L, Franz L, Min M, Bachmann R, Martens U, Stanek K, Stübner K, Nelson BK, Herrmann U, Weber B, López-Martínez M, Jonckheere R, Sperner B, Tichomirowa M, Mcwilliams MO, Gordon M, Meschede M and Bock P (2009) The North American-Caribbean Plate boundary in Mexico-Guatemala-Honduras. *Geological Society, London, Special Publications* **328**(1), 219–93.

Restrepo-Pace PA, Ruiz J, Gehrels G and Cosca M (1997) Geochronology and Nd isotopic data of Grenville-age rocks in the Colombian Andes: new constraints for Late Proterozoic-Early Paleozoic paleocontinental reconstructions of the Americas. *Earth and Planetary Science Letters* **150**(3), 427–41.

Rogers RD and Mann P (2007) Transtensional deformation of the western Caribbean–North America plate boundary zone.

Rubio-Cisneros II and Lawton TF (2011) Detrital zircon U-Pb ages of sandstones in continental red beds at Valle de Huizachal, Tamaulipas, NE Mexico: record of early-middle Jurassic arc volcanism and transition to crustal extension. *Geosphere* **7**(1), 159–70.

Ruiz J, Patchett PJ and Ortega-Gutiérrez F (1988) Proterozoic and Phanerozoic basement terranes of Mexico from Nd isotopic studies. *GSA Bulletin* **100**(2), 274–81.

Scherer E, Münker C and Mezger K (2001) Calibration of the Lutetium-Hafnium Clock. *Science* **293**(5530), 683–87.

Söderlund U, Patchett PJ, Vervoort JD and Isachsen CE (2004) The 176Lu decay constant determined by Lu–Hf and U–Pb isotope systematics of Precambrian mafic intrusions. *Earth and Planetary Science Letters* **219**(3), 311–24.

Solari LA, Keppie JD, Ortega-Gutiérrez F, Cameron KL, Lopez R and Hames, W.E. (2003) 990 and 1100 Ma Grenvillian tectonothermal events in the northern Oaxacan Complex, southern Mexico: roots of an orogen. *Tectonophysics* **365**(1), 257–82.

Solari LA, Ortega-Gutiérrez F, Elías-Herrera M, Schaaf P, Norman M, De León RT, Ortega-Obregón C, Chiquín M and Ical SM (2009) U-Pb zircon geochronology of Palaeozoic units in Western and Central Guatemala: insights into the tectonic evolution of middle America. *Geological Society, London, Special Publications* **328**(1), 295–313.

Solari LA, Tuena AG, Gutíerrez FO and Obregón CO (2011) The Chuacús Metamorphic complex, central Guatemala: geochronological and geochemical constraints on its Paleozoic - Mesozoic evolution. *Geologica acta*, 329–50.

Solari LA, García-Casco A, Martens U, Lee, JKW and Ortega-Rivera A (2013) Late Cretaceous subduction of the continental basement of the maya block (Rabinal Granite, central Guatemala): Tectonic implications for the geodynamic evolution of Central America. *GSA Bulletin* **125**(3–4), 625–39.

Spikings R, Reitsma MJ, Boekhout F, Mišković A, Ulianov A, Chiaradia M, Gerdes A and Schaltegger U (2016) Characterisation of Triassic rifting in Peru and implications for the early disassembly of western Pangaea. *Gondwana Research* **35**, 124–43.

Sylvester PJ (1998) Post-collisional strongly peraluminous granites. *Lithos* **45**(1), 29–44.

Talavera-Mendoza O, Ruiz J, Gehrels GE, Meza-Figueroa DM, Vega-Granillo R and Campa-Uranga MF (2005) U–Pb geochronology of the Acatlán complex and implications for the Paleozoic paleogeography and tectonic evolution of southern Mexico. *Earth and Planetary Science Letters* **235**(3), 682–99.

Tazzo-Rangel MD, Weber B, González-Guzmán R, Valencia VA, Frei D, Schaaf P and Solari LA (2019) Multiple metamorphic events in the Palaeozoic Mérida Andes basement, venezuela: insights from U–Pb geochronology and Hf–Nd isotope systematics. *International Geology Review* **61**(13), 1557–93.

Teixeira W, Geraldes MC, Matos R, Ruiz AS, Saes G and Vargas-Mattos G (2010) A review of the tectonic evolution of the Sunsás belt, SW Amazonian Craton. *Journal of South American Earth Sciences* **29**(1), 47–60.

Torres De León R, Solari LA, Ortega-Gutiérrez F and Martens U (2012) The Chortís Block—southwestern México connections: U-Pb zircon geochronology constraints. *American Journal of Science* **312**(3), 288–313.

Tsujimori T, Sisson VB, Liou JG, Harlow GE and Sorensen SS (2006) Petrologic characterization of Guatemalan lawsonite eclogite: Eclogitization of subducted oceanic crust in a cold subduction zone. In *Ultrahigh-pressure metamorphism: Deep continental subduction* (eds BR Hacker, WC McClelland and JG Liou). Geological Society of America Special Paper **403**, 147–168.

Valencia-Morales YT, Weber B, Tazzo-Rangel MD, González-Guzmán R, Frei D, Quintana-Delgado JA and Rivera-Moreno EN (2022) Early Mesoproterozoic inliers in the chiapas massif complex of southern Mexico: Implications on Oaxaquia-Amazonia-Baltica configuration. *Precambrian Research* **373**, 106611.

Vermeesch P (2012) On the visualisation of detrital age distributions. *Chemical Geology* **312–313**, 190–94.

Vermeesch P (2021) On the treatment of discordant detrital zircon U–Pb data. *Geochronology* **3**(1), 247–57.

Vervoort JD, Patchett PJ, Albarède F, Blichert-Toft J, Rudnick R and Downes, H. (2000) Hf–Nd isotopic evolution of the lower crust. *Earth and Planetary Science Letters* **181**(1), 115–29.

Vervoort JD, Plank T and Prytulak J (2011) The Hf–Nd isotopic composition of marine sediments. *Geochimica et Cosmochimica Acta* **75**(20), 5903–26.

Weber B and Köhler H (1999) Sm–Nd, Rb–Sr and U–Pb geochronology of a Grenville Terrane in Southern Mexico: origin and geologic history of the Guichicovi Complex. *Precambrian Research* **96**(3), 245–62.

Weber B, Valencia VA, Schaaf P, Pompa-Mera V and Ruiz J (2008) Significance of provenance ages from the chiapas massif complex (Southeastern Mexico): Redefining the Paleozoic basement of the maya block and its evolution in a Peri-Gondwanan Realm. *The Journal of Geology* **116**(6), 619–39.

Weber B, Valencia VA, Schaaf P and Ortega-Gutiérrez F (2009) Detrital zircon ages from the lower santa rosa formation, chiapas: implications on regional Paleozoic stratigraphy. *Revista mexicana de ciencias geológicas* **26**(1), 260–76.

Weber B, Scherer EE, Schulze C, Valencia VA, Montecinos P, Mezger K and Ruiz, J. (2010) U–Pb and Lu–Hf isotope systematics of lower crust from central-southern Mexico – geodynamic significance of Oaxaquia in a Rodinia Realm. *Precambrian Research* **182**(1), 149–62.

Weber B, Scherer EE, Martens UK and Mezger K (2012) Where did the lower Paleozoic rocks of Yucatan come from? A U–Pb, Lu–Hf, and Sm–Nd isotope study. *Chemical Geology* **312–313**, 1–17.

Weber B, González-Guzmán R, Manjarrez-Juárez R, Cisneros De León A, Martens U, Solari L, Hecht L and Valencia V (2018) Late Mesoproterozoic to Early Paleozoic history of metamorphic basement from the southeastern chiapas massif complex, Mexico, and implications for the evolution of NW Gondwana. *Lithos* **300–301**, 177–99.

Whalen JB, Currie KL and Chappell BW (1987) A-type granites: geochemical characteristics, discrimination and petrogenesis. *Contributions to Mineralogy and Petrology*, **95**(4), 407–19.

Yui T-F, Maki K, Usuki T, Lan C-Y, Martens U, Wu C-M, Wu T-W and Liou JG (2010) Genesis of Guatemala jadeitite and related fluid characteristics: Insight from zircon. *Chemical Geology* **270**(1), 45–55.